Nonlinear finite volume discretization for transient diffusion problems on general meshes

El Houssaine Quenjel

▶ **To cite this version:**

El Houssaine Quenjel. Nonlinear finite volume discretization for transient diffusion problems on general meshes. Applied Numerical Mathematics, 2021, 161, pp.148 - 168. 10.1016/j.apnum.2020.11.001 . hal-03492828

HAL Id: hal-03492828
https://hal.science/hal-03492828

Submitted on 21 Nov 2022

HAL is a multi-disciplinary open access archive for the deposit and dissemination of scientific research documents, whether they are published or not. The documents may come from teaching and research institutions in France or abroad, or from public or private research centers.

L'archive ouverte pluridisciplinaire **HAL**, est destinée au dépôt et à la diffusion de documents scientifiques de niveau recherche, publiés ou non, émanant des établissements d'enseignement et de recherche français ou étrangers, des laboratoires publics ou privés.

Distributed under a Creative Commons Attribution - NonCommercial 4.0 International License

Version of Record: https://www.sciencedirect.com/science/article/pii/S0168927420303512
Manuscript_e2498ce8889e7e95d8cbb72aa2e2f2e9

Nonlinear finite volume discretization for transient diffusion problems on general meshes

El Houssaine Quenjel

Université Côte d'Azur, Inria, CNRS, LJAD, Coffee Team, Parc Valrose, 06108 Nice cedex 02, France.
quenjel@unice.fr

October 23, 2020

Abstract

A nonlinear discrete duality finite volume scheme is proposed for time-dependent diffusion equations. The model example is written in a new formulation giving rise to similar nonlinearities for both the diffusion and the potential functions. A natural finite volume discretization is built on this particular problem's structure. The fluxes are generically approximated thanks to a key fractional average. The point of this strategy is to promote coercivity and scheme's stability simultaneously. The existence of positive solutions is guaranteed. The theoretical convergence of the nonlinear scheme is established using practical compactness tools. Numerical results are performed in order to highlight the second order accuracy of the methodology and the positiveness of solutions on distorted meshes.

Key words : nonlinear diffusion equations, discrete duality finite volume scheme, coercivity, positivity, convergence, second order accuracy.

AMS subject classifications : 35K55, 35K65, 65M08, 65M12.

1 Introduction

We consider $Q_{t_f} = \Omega \times (0, t_f)$ where Ω is a bounded connected open subset of $\mathbb{R}^d$ ($d \in \mathbb{N}^*$) and $t_f > 0$ refers to the time. A transient nonlinear diffusion process can be represented with the parabolic equation

$$\frac{\partial p}{\partial t} - \operatorname{div} \mu(p)\Lambda\nabla p = 0 \quad \text{in} \quad Q_{t_f}, \tag{1.1}$$

whose main unknown is p which could account for a saturation of fluid, temperature of material or density of population. The function $\mu(p)$ measures the behavior of nonlinear dispersion of p in Ω. The matrix Λ provides preferential axes along which strong or weak diffusion could take place. A complete description of such a process necessitates some specific closure constraints. In our case, it is given by the homogeneous Neumann boundary condition

$$\mu(p)\Lambda\nabla p \cdot \mathbf{n} = 0 \quad \text{on} \quad \partial\Omega \times (0, t_f), \tag{1.2}$$

where $\mathbf{n}$ is the outward unit normal to the domain boundary $\partial\Omega$. To start this time-dependent problem, we specify the initial datum by

$$p(\cdot, 0) = p^0 \quad \text{in} \quad \Omega. \tag{1.3}$$

In this contribution, the construction of the numerical scheme relies heavily on a nonstandard reformulation of the above problem. It requires by the way the useful Kirchhoff transform

$$\zeta(p) = \int_0^p \mu(a)\,\mathrm{d}a. \tag{1.4}$$

© 2020 published by Elsevier. This manuscript is made available under the CC BY NC user license
https://creativecommons.org/licenses/by-nc/4.0/

Therefore, (1.1) can be formally presented in the following equivalent form

$$\frac{\partial p}{\partial t} - 2\,\mathrm{div}\,\sqrt{\zeta(p)}\Lambda\nabla\sqrt{\zeta(p)} = 0.$$

By setting $\beta(p) = \sqrt{2\zeta(p)}$, the previous equality reads

$$\frac{\partial p}{\partial t} - \mathrm{div}\,\beta(p)\Lambda\nabla\beta(p) = 0. \tag{1.5}$$

Next we write the main hypotheses that must be imposed on the different data involved in our model problem in order to properly give the meaning of the sought solution.

(i) β is a continuous and strictly increasing function from $\mathbb{R}^+$ into $\mathbb{R}^+$ such that $\beta(0) = 0$ and $\beta(s) > 0$ for all $s \in (0, +\infty)$.

(ii) The tensor Λ is a symmetric matrix of $L^\infty(\Omega)^{d\times d}$ such that there exist two constants $\underline{\Lambda} > 0$ and $\overline{\Lambda}$ with

$$\underline{\Lambda}\,|v|^2 \leq \Lambda(x)v\cdot v \leq \overline{\Lambda}\,|v|^2 \quad \text{a.e. } x \in \Omega \text{ and } \forall v \in \mathbb{R}^d.$$

(iii) Let us consider Υ a nonnegative primitive of $u \mapsto \log(\beta(u))$ that will subsequently be said the entropy. By construction, the function Υ is convex. We assume the following items.

(a) The initial state p^0 is a nonnegative function of $L^1(\Omega)$ with a positive mass i.e. $\displaystyle\int_\Omega p^0\,\mathrm{d}x > 0$. We also need a control on the initial entropy function in the following sense

$$0 \leq \int_\Omega \Upsilon(p^0(x))\,\mathrm{d}x < +\infty. \tag{1.6}$$

(b) We require an asymptotic behavior on Υ as follows

$$\frac{\Upsilon(s)}{s} \longrightarrow +\infty \quad \text{and} \quad \frac{\Upsilon(s)}{\beta(s)^2} \longrightarrow +\infty \quad \textit{as} \quad s \longrightarrow +\infty. \tag{1.7}$$

Remark 1.1. *Let us construct an example of the entropy Υ. To this end, we fix some $\gamma > 0$ and set $C_\gamma = \dfrac{\gamma+1}{2}$. We next consider*

$$\mu(s) = \begin{cases} C_\gamma s^\gamma & \textit{if } s \leq 1 \\ C_\gamma & \textit{if } s > 1 \end{cases}.$$

By definition of β, one computes

$$\beta(s) = \begin{cases} s^{C_\gamma} & \textit{if } s \leq 1 \\ \sqrt{2C_\gamma s - \gamma} & \textit{if } s > 1 \end{cases}.$$

Then, the entropy function verifying (1.7) can be taken as

$$\Upsilon(s) = \begin{cases} C_\gamma(s\log(s) - s + 1) & \textit{if } s \leq 1 \\ \dfrac{1}{2}\Big(X(s)\log(X(s)) - X(s) + 1\Big) & \textit{if } s > 1 \end{cases},$$

where $X(s) = 2C_\gamma s - \gamma$. Up to a modification enabling the continuity of μ, note that if $\mu(s)$ fits a bounded function when $s \to +\infty$ then (1.7) is automatically satisfied. The latter situation generally occurs in practice.

The following statement defines the notion of a weak solution to the considered problem. Note that the existence of such a weak solution to the model problem (1.1)-(1.3) in the sense below was the object of the work [3]. The convergence of the proposed numerical scheme is an alternative way to prove the existence result.

Definition 1.1. *Let us assume that the items **(i)-(iii)** are fulfilled. A measurable function $p : Q_{t_f} \longrightarrow (0, +\infty)$ is called a weak solution to the continuous model* (1.1)-(1.3) *if $\Upsilon(p) \in L^\infty(0, t_f; L^1(\Omega))$, $\beta(p) \in L^2(0, t_f; H^1(\Omega))$ and p solves the integral formulation*

$$-\int_{Q_{t_f}} p\frac{\partial\psi}{\partial t}\,\mathrm{d}x\,\mathrm{d}t - \int_\Omega p^0\psi(\cdot,0)\,\mathrm{d}x + \int_{Q_{tf}} \beta(p)\Lambda\nabla\beta(p)\cdot\nabla\psi\,\mathrm{d}x\,\mathrm{d}t = 0,\ \ \forall\psi \in \mathcal{C}_c^\infty(\overline{\Omega}\times[0,t_f)). \tag{1.8}$$

Diffusion equations of type (1.1) arise widely in a lot of mathematical and physical problems modeling complex flows in porous media [23], heat transfer in materials [42], and biological processes [41, 38]. Various computational methods with specific goals, like consistency, stability, accuracy etc, have been devoted to the discretization of problems recast in the formulation (1.1). In addition to the finite element literature [4, 9, 30, 47], it is well established that many finite volume methods provide consistent and accurate approximations to diffusion terms. By consistency we mean the convergence of the discrete fluxes towards their continuous counterparts in the weak sense. There exists a rich documentation on the finite volume approximation. The most famous finite volume method is TPFA (Two-Point Flux Approximation). The TPFA like schemes are widely used in practice due to their efficient local computation of the fluxes and cheap implementation. They have been intensively analyzed in a great number of contributions [2, 6, 10, 21, 31, 33, 35]. In order to take into consideration anisotropic and heterogeneous fields, multi-point approximation of the fluxes is mandatory. For this reason, the Hybrid Mimetic Mixed (HMM) schemes have been conceived and analyzed in [1, 17, 28, 32]. Also, the Vertex Approximate Gradient (VAG) methods [15, 34] have shown a privileged performance in capturing as accurately as possible the solution jumps in the presence of highly heterogeneous fields. Additionally, the Discrete Duality Finite Volume (DDFV) approach [5, 7, 14, 24, 25, 26, 40, 43] is a natural extension of the TPFA method to complex situations. A comparison of the aforementioned discretizations as well as other ones has been carried out in the review [27]. Most of the described methods have shown to fit in the abstract framework [29] referred to as the gradient discretization method.

We would like to emphasize that in porous media flow type problems for instance, relevant functions like the approximate saturation or the temperature must stay in the physical ranges so that it can be physically admissible. To address this requirement a few positive and consistent schemes have been developed and examined in the recent past years [15, 16, 19, 37, 36, 45]. The point is about the elimination of possible oscillations using appropriate first order upwind schemes for the diffusion like in the case of convection. A different approach was suggested in [20, 18] where the authors exploited the features of some singular functions near zero to achieve higher-positive resolutions. Being inspired by [20] we have suggested an accurate and robust finite volume finite element approximation with respect to the anisotropy in the case of a linear elliptic operator [44] with a linear transport. Hence, there is a strong interest in designing new reliable discretizations coupling between stability, accuracy and positivity for complex problems. To this end, we are going to extend the methodology of [44] to more general nonlinearities of $\beta(p)$ with weakest assumptions.

In this work we stick to a strategy preserving the original (quadratic) accuracy of the finite volume method. Then, one retains an easy updating of already existing codes without modifying the stencil or the core of the method. Our scheme is constructed using the DDFV framework. As advantages of the DDFV method, it enjoys a discrete Stokes formula allowing for the establishment of readily a priori analysis, especially the unconditional coercivity, as in the continuous setting. It is further a pure finite volume approximation that uses relevant and peculiar unknowns per each control volume interface. The method has been shown to be accurate of second order and efficient for anisotropic diffusion problems on general meshes through many various tests of the famous FVCA benchmark [39]. As a relative drawback, the DDFV methodology lacks positivity or a discrete maximum principle on general meshes and anisotropies. The latter is obviously fulfilled under restrictive assumptions placed on the mesh or on the tensor Λ. In a general context we proposed in [46] an alternative correction to the finite volume scheme so that one can recover the discrete maximum principle. Although the approach provided in [46] seems to be quite

general, the scheme turns out to be accurate for smooth analytical solutions. It further exhibits low accuracy when the exact solution is merely continuous because of the upwinding. Therefore to make use of the aforementioned attractive features of DDFV approximation, it is highly desirable to circumvent the positivity issue.

Motivated by the above strengths, we propose in this contribution an attempt to devise a reliable nonlinear DDFV scheme to approximate the weak solution to the model equation (1.1). The first idea is to take advantage of the nonlinear formulation (1.5) allowing a symmetric distribution of the problem nonlinearity. After carrying out a finite volume discretization on the primal and dual meshes, the second key point relies on the approximation of the fluxes. It consists of a fractional centered mean of the new diffusion coefficient termed by $\beta(p)$. These elements are sufficient to derive energy estimates and claim that the scheme is positivity preserving. The numerical scheme should be convergent not only for few assumptions, allowing particular (smooth) solutions, but for any type of solution respecting the weakest Assumptions **(i)-(iii)**. This fact is established by means of a compactness criterion. The theoretical scheme is implemented and run on several test cases. The purpose is to assess the method's accuracy and check the numerical solution positivity in the case of distorted meshes and in the presence of anisotropy.

The rest of this work is outlined as follows. In Section 2 we first specify the meshes in the DDFV context. We survey the construction of the discrete functions and operators as well as discrete norms. We next develop a generic finite volume scheme. A priori estimations are derived in Section 3, which are elements of great importance to prove the existence of positive solutions. Combining these ingredients with compactness arguments we prove the convergence of the nonlinear finite volume scheme in Section 4. Results of scheme's implementation are discussed in Section 5. A summary of the paper is given in Section 6.

2 Nonlinear discrete duality finite volume approximation

Before exposing the numerical scheme, we should first specify the meshes, especially the spatial discretization of the domain Ω, and the discrete operators in the context of the DDFV framework. We stick to the two dimensional case to highlight the point of the proposed methodology.

2.1 Mesh setting and discrete operators

As a finite volume discretization, the construction of the DDFV fluxes across interfaces are built from the connectivity lists of the primal mesh, the dual mesh and the diamond mesh. We denote $\overline{\mathfrak{M}} = \mathfrak{M} \cup \partial\mathfrak{M}$ as the primal mesh consisting of a collection of internal polygonal subsets $\mathfrak{M}$, together with external edges considered as degenerate cells $\partial\mathfrak{M}$. Each subset $A \in \overline{\mathfrak{M}}$ is referred to as a primal control volume. The union of the control volumes covers the whole domain Ω. This partition generates a finite set of edges denoted by $\mathcal{E}$ as well as a family of points $\{x_A\}_{A\in\overline{\mathfrak{M}}}$ called primal "centers" such that $x_A \in A$ for all $A \in \overline{\mathfrak{M}}$. For instance, one can take the point x_A as the barycenter of A. The diameter of A is denoted by h_A and its volume by $|A|$. We write $\mathcal{E}_A$ the set containing the edges of the cell A. We denote $|\sigma|$ as the length of $\sigma \in \mathcal{E}_A$. The unit normal to $\sigma \in \mathcal{E}_A$ outwards A is denoted by $\mathbf{n}_{\sigma,A}$.

The dual mesh $\overline{\mathfrak{M}^\star} = \mathfrak{M}^\star \cup \partial\mathfrak{M}^\star$ is devised around the vertices of the primal one and it covers in its turn the domain Ω. To each vertex $x_{A^\star}$ of $\overline{\mathfrak{M}}$ we associate a unique dual control volume $A^\star \in \overline{\mathfrak{M}^\star}$. It is set up by connecting the mass centers of the primal cells having in common $x_{A^\star}$ as a vertex. We hereafter call these vertices the dual centers. We denote the diameter of $A^\star$ by $h_{A^\star}$ and its volume by $|A^\star|$. The edges of $\overline{\mathfrak{M}^\star}$ are gathered in the set $\mathcal{E}^\star$. Let $|\sigma^\star|$ denote the length of the dual edge $\sigma^\star \in \mathcal{E}^\star$. The unit normal to $\sigma^\star \in \mathcal{E}^\star_{A^\star}$ outwards to $A^\star$ is denoted by $\mathbf{n}_{\sigma^\star,A^\star}$.

The diamond mesh $\mathfrak{S} = \mathfrak{S}_{\rm int} \cup \mathfrak{S}_{\rm ext}$ is a third decomposition of Ω which is obtained using the primal edges. Indeed, for every internal primal edge $\sigma = A|B \in \mathcal{E}$ shared by $A, B \in \mathfrak{M}$, we associate a unique dual edge $\sigma^\star = A^\star|B^\star \in \mathcal{E}^\star$ shared by $A^\star, B^\star \in \overline{\mathfrak{M}^\star}$. These two entities define the main diagonals of the internal diamond $\mathcal{D}_{\sigma,\sigma^\star} \in \mathfrak{S}_{\rm int}$. Any boundary diamond $\mathcal{D}_{\sigma,\sigma*} \in \mathfrak{S}_{\rm ext}$ is prescribed by the triangle given by the center and the edge $\sigma \in \mathcal{E}^{\rm ext}$ of some primal cell. Note that this center is an extremity of σ^*. Rearranging in a circular way the vertices x_A, x_B of σ and the vertices $x^\star_A, x^\star_B$ of $\sigma^\star$ we get those of $\mathcal{D}_{\sigma,\sigma^\star} \in \mathfrak{S}$. Let $x_A, x^\star_A, x_B, x^\star_B$ be the vertices of $D_{\sigma,\sigma^\star}$. Let $\mathbf{t}_{A,B}$ be the unit tangent vector to the primal edge $\sigma = A|B$

oriented from A to B. In an analogous way, we define $\mathbf{t}_{A^\star,B^\star}$ the unit tangent vector to $\sigma^\star = A^\star|B^\star$. These two vectors are so that the couples $(\mathbf{n}_{\sigma^\star,A^\star}, \mathbf{t}_{A,B})$ and $(\mathbf{t}_{A^\star,B^\star}, \mathbf{n}_{\sigma^\star,A^\star})$ constitute direct bases. Let $\alpha_\mathcal{D}$ in $]0,\pi/2]$ stand for the angle provided by the two directions (A,B) and $(A^\star,B^\star)$. We refer to $h_\mathcal{D}$ as the diameter of $\mathcal{D} \in \mathfrak{S}$ and we set $h = \max_{\mathcal{D}\in\mathfrak{S}} h_\mathcal{D}$. We denote $|\mathcal{D}|$ the volume of the diamond $\mathcal{D} \in \mathfrak{S}$. It is computed using the elementary equality

$$|\mathcal{D}| = \frac{1}{2}\,|\sigma|\,|\sigma^\star|\sin(\alpha_\mathcal{D}). \tag{2.1}$$

We refer to Figure 1 for an illustration of the aforementioned geometrical objects. We further need to

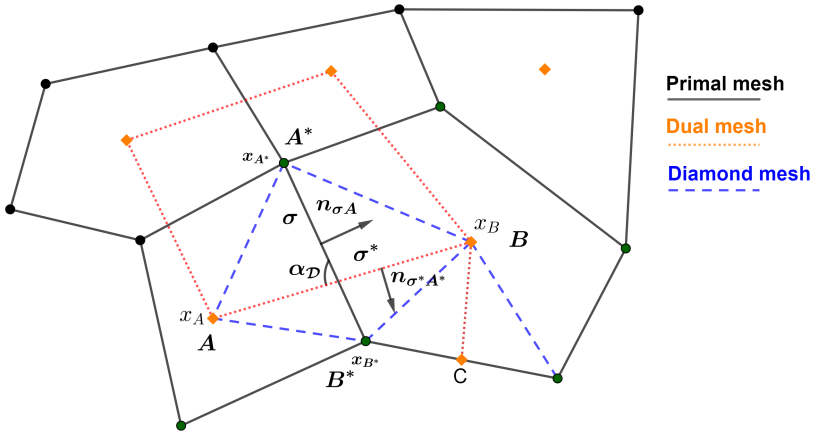

Figure 1: Primal control volumes A, B and dual cells $A^\star, B^\star$ as well as the units normal vectors $\mathbf{n}_{\sigma,A}, \mathbf{n}_{\sigma^\star,A^\star}$ to σ and $\sigma^\star$. The cell C reduces to a single boundary edge. The blue dashed region is the diamond cell.

suppose a regularity requirement on the mesh to control in particular the flatting of the diamond cells. The mesh regularity is defined by

$$\theta^\mathcal{D} = \max\left(\frac{1}{\sin(\alpha_\mathcal{D})}, \frac{h_\mathcal{D}}{\sqrt{|\mathcal{D}|}}, \max_{K=A,B}\frac{h_K}{\sqrt{|K|}}, \max_{K^\star=A^\star,B^\star}\frac{h_{K^\star}}{\sqrt{|K^\star|}}\right).$$

In the rest of this paper we assume that there exist constants $\underline{\theta}, \overline{\theta} > 0$ such that

$$\underline{\theta} \le \theta^\mathcal{D} \le \overline{\theta}, \quad \forall \mathcal{D} \in \mathfrak{S}. \tag{2.2}$$

We consider $\mathbb{R}^\mathcal{T}$ the space where the primal and dual unknowns live. We will sometimes writes $v_\mathcal{T} \in (\mathbb{R}_{+,*})^\mathcal{T}$ meaning that all components of $v_\mathcal{T}$ are positive. The set $\mathbb{R}^\mathcal{T}$ contains elements of the form

$$v_\mathcal{T} = \Big((v_A)_{A\in\overline{\mathfrak{M}}}, (v_{A^\star})_{A^\star\in\overline{\mathfrak{M}^\star}}\Big).$$

It is moreover endowed with the bilinear form

$$[\![v_\mathcal{T}, w_\mathcal{T}]\!]_\mathcal{T} = \frac{1}{2}\sum_{A\in\mathfrak{M}} |A|\,v_A w_A + \frac{1}{2}\sum_{A\in\overline{\mathfrak{M}}} |A^\star|\,v_{A^\star} w_{A^\star}.$$

It is positive, but not necessary definite since the degenerate boundary cells of $\partial\mathfrak{M}$ are missing.

If g is a nonlinear function from $\mathbb{R}$ into $\mathbb{R}$ we denote $g(v_\mathcal{T})$ the element of $\mathbb{R}^\mathcal{T}$ defined by

$$g(v_\mathcal{T}) = \Big((g(v_A))_{A\in\overline{\mathfrak{M}}}, (g(v_{A^\star}))_{A^\star\in\overline{\mathfrak{M}^\star}}\Big).$$

Performing the convergence analysis of the scheme requires to introduce reconstruction functions which are piecewise constant on the primal and dual meshes. Given a vector $v_{\mathcal{T}} \in \mathbb{R}^{\mathcal{T}}$ we define

$$v_{\mathfrak{M}}(x) = v_A \quad \forall x \in A,\ \forall A \in \mathfrak{M}, \quad v_{\overline{\mathfrak{M}^\star}}(x) = v_{A^\star} \quad \forall x \in A^\star,\ \forall A^\star \in \overline{\mathfrak{M}^\star},$$

which are identified to two elements of $L^2(\Omega)$. We also define the $L^2(\Omega)$-function v_h that combines both $v_{\mathfrak{M}}$ and $v_{\overline{\mathfrak{M}^\star}}$ such that

$$v_h = \frac{1}{2}(v_{\mathfrak{M}} + v_{\overline{\mathfrak{M}^\star}}).$$

On the other hand, the DDFV approach is characterized by the definition of a particular discrete gradient which is built on the diamond mesh in a piecewise manner. Then for every $v_{\mathcal{T}} \in \mathbb{R}^{\mathcal{T}}$ we define in each diamond cell

$$\nabla_{\mathcal{D}} v_{\mathcal{T}} = \frac{1}{\sin(\alpha_{\mathcal{D}})} \left(\frac{v_B - v_A}{|\sigma^\star|} \mathbf{n}_{\sigma,A} + \frac{v_{B^\star} - v_{A^\star}}{|\sigma|} \mathbf{n}_{\sigma^\star,A^\star} \right), \quad \forall \mathcal{D} \in \mathfrak{S}. \tag{2.3}$$

We can therefore reconstruct the gradient operator denoted by $\nabla_{\mathfrak{S}}$ as follows

$$\nabla_{\mathfrak{S}} v_{\mathcal{T}}(x) = \nabla_{\mathcal{D}} v_{\mathcal{T}} \quad \forall x \in \mathcal{D},\ \forall \mathcal{D} \in \mathfrak{S},$$

which is in its turn a function of $L^2(\Omega)^2$. This discrete gradient is consistent in the strong sense because it is constructed on both directions : the primal and dual normal vectors giving rise to a basis of $\mathbb{R}^2$. In practice we consider the following equivalent formula of the discrete gradient instead of the above one (2.3). It is obtained by virtue of (2.1)

$$\nabla_{\mathcal{D}} v_{\mathcal{T}} = \frac{1}{2\,|\mathcal{D}|} \Big(|\sigma|\,(v_B - v_A)\,\mathbf{n}_{\sigma,A} + |\sigma^\star|\,(v_{B^\star} - v_{A^\star})\,\mathbf{n}_{\sigma^\star,A^\star} \Big), \quad \forall \mathcal{D} \in \mathfrak{S}. \tag{2.4}$$

Hence, one has

$$|\mathcal{D}|\,|\nabla_{\mathcal{D}} v_{\mathcal{T}}|^2 = \delta_{\mathcal{D}} v_{\mathcal{T}} \cdot \mathbb{K}_{\mathcal{D}} \delta_{\mathcal{D}} v_{\mathcal{T}}, \quad \forall \mathcal{D} \in \mathfrak{S},$$

where we set

$$\delta_{\mathcal{D}} v_{\mathcal{T}} = \begin{pmatrix} v_A - v_B \\ v_{A^\star} - v_{B^\star} \end{pmatrix},$$

and

$$\mathbb{K}_{\mathcal{D}} = \frac{1}{4\,|\mathcal{D}|} \begin{pmatrix} |\sigma|^2 & |\sigma|\,|\sigma^\star|\,\mathbf{n}_{\sigma,A} \cdot \mathbf{n}_{\sigma^\star,A^\star} \\ |\sigma|\,|\sigma^\star|\,\mathbf{n}_{\sigma,A} \cdot \mathbf{n}_{\sigma^\star,A^\star} & |\sigma^\star|^2 \end{pmatrix}.$$

The following result shows that this local matrix is symmetric and positive-definite.

Lemma 2.1. *There exist positive constant C_1, C_2 depending only on the mesh regularity such that*

$$C_1\,|w|^2 \le \mathbb{K}_{\mathcal{D}} w \cdot w \le C_2\,|w|^2, \quad \forall w = (w_1, w_2) \in \mathbb{R}^2, \quad \forall \mathcal{D} \in \mathfrak{S}.$$

Proof. First, we observe that

$$\begin{aligned} \mathbb{K}_{\mathcal{D}} w \cdot w &= \frac{1}{4\,|\mathcal{D}|} \left(w_1^2\,|\sigma|^2 + 2 w_1 w_2\,|\sigma|\,|\sigma^\star|\,\mathbf{n}_{\sigma,A} \cdot \mathbf{n}_{\sigma^\star,A^\star} + w_2^2\,|\sigma^\star|^2 \right) \\ &\ge \frac{1}{4\,|\mathcal{D}|} \left(w_1^2\,|\sigma|^2 - 2\,|w_1|\,|\sigma|\,|w_2|\,|\sigma^\star|\,|\mathbf{n}_{\sigma,A} \cdot \mathbf{n}_{\sigma^\star,A^\star}| + w_2^2\,|\sigma^\star|^2 \right) \\ &\ge \frac{1}{4\,|\mathcal{D}|} \Big(w_1^2\,|\sigma|^2 - (w_1^2\,|\sigma|^2 + w_2^2\,|\sigma^\star|^2)\,|\mathbf{n}_{\sigma,A} \cdot \mathbf{n}_{\sigma^\star,A^\star}| + w_2^2\,|\sigma^\star|^2 \Big). \end{aligned}$$

Thanks to the regularity assumption on the mesh (2.2) there exists $\underline{\alpha} \in]0, \pi/2]$ such that

$$|\mathbf{n}_{\sigma,A} \cdot \mathbf{n}_{\sigma^\star,A^\star}| = |\cos(\alpha_{\mathcal{D}})| \le \cos(\underline{\alpha}) < 1, \quad \forall \mathcal{D} \in \mathfrak{S}.$$

Using the fact that $\dfrac{h_{\mathcal{D}}^2}{\overline{\theta}^2} \le |\mathcal{D}| \le |\sigma|\,|\sigma^\star|$ gives $|\sigma| \le \overline{\theta}^2\,|\sigma^\star|$ and $|\sigma^\star| \le \overline{\theta}^2\,|\sigma|$. Hence, one has

$$\frac{|\sigma|^2}{|\mathcal{D}|} \ge \frac{|\sigma|}{|\sigma^\star|} \ge \frac{1}{\overline{\theta}^2}, \quad \frac{|\sigma^\star|^2}{|\mathcal{D}|} \ge \frac{|\sigma^\star|}{|\sigma|} \ge \frac{1}{\overline{\theta}^2}.$$

As a consequence

$$\mathbb{K}_{\mathcal{D}} w \cdot w \geq \frac{1-\cos(\underline{\alpha})}{4\,|\mathcal{D}|}\left(w_1^2\,|\sigma|^2 + w_2^2\,|\sigma^\star|^2\right) \geq C_1\,|w|^2\,, \quad \forall \mathcal{D} \in \mathfrak{S},\ \text{with } C_1 = \frac{1-\cos(\underline{\alpha})}{4\overline{\theta}^2}.$$

Again, from the mesh shape condition (2.2), we have that $|\sigma|\,, |\sigma^\star| \leq \overline{\theta}\sqrt{|\mathcal{D}|}$. Then, we directly estimate

$$\mathbb{K}_{\mathcal{D}} w \cdot w = \frac{1}{4\,|\mathcal{D}|}\left(w_1^2\,|\sigma|^2 + 2w_1 w_2\,|\sigma|\,|\sigma^\star|\,\mathbf{n}_{\sigma,A}\cdot\mathbf{n}_{\sigma^\star,A^\star} + w_2^2\,|\sigma^\star|^2\right) \leq C_2\,|w|^2\,,$$

where $C_2 = \overline{\theta}^2/2$. □

Note that the primal and dual unknowns are only connected in the discrete gradient expression. A priori, it is not known how to link their corresponding reconstructions $v_{\mathfrak{M}}, v_{\overline{\mathfrak{M}^\star}}$, at least to the discrete gradient. This sort of fact is essentially required to show that these functions tend indeed to the same limit when the mesh size goes to 0 from a theoretical viewpoint. A possible way to reinforce this convergence is to incorporate a penalization term in the numerical scheme so that one ultimately recovers (formally) an inequality of type

$$\left\|v_{\overline{\mathfrak{M}^\star}} - v_{\mathfrak{M}}\right\|_{L^2(\Omega)} \leq Ch\,\|\nabla_{\mathfrak{S}} v_{\mathcal{T}}\|_{L^2(\Omega)^2}\,,$$

for some $C > 0$ that depends only on the data and on the geometrical regularity of the mesh. Following [5], the penalty operator $\mathcal{P}^{\mathcal{T}} : \mathbb{R}^{\mathcal{T}} \to \mathbb{R}^{\mathcal{T}}$ which maps $v_{\mathcal{T}}$ to $\mathcal{P}^{\mathcal{T}} v_{\mathcal{T}} = w_{\mathcal{T}}$ is defined per components by

$$w_A = \frac{1}{|A|}\frac{1}{h^\eta}\sum_{A^\star \in \overline{\mathfrak{M}^\star}} |A \cap A^\star|\,(v_A - v_{A^\star}), \quad \forall A \in \mathfrak{M}, \quad w_A = 0, \quad \forall A \in \partial\mathfrak{M},$$
$$w_{A^\star} = \frac{1}{|A^\star|}\frac{1}{h^\eta}\sum_{A \in \mathfrak{M}} |A \cap A^\star|\,(v_{A^\star} - v_A), \quad \forall A^\star \in \overline{\mathfrak{M}^\star},$$

where $\eta \in (0,2)$ is a given parameter. Then, one establishes the identity

$$\left[\!\left[\mathcal{P}^{\mathcal{T}} v_{\mathcal{T}}, u_{\mathcal{T}}\right]\!\right]_{\mathcal{T}} = \frac{1}{2}\frac{1}{h^\eta}\sum_{A \in \mathfrak{M}}\sum_{A^\star \in \overline{\mathfrak{M}^\star}} |A \cap A^\star|\,(v_A - v_{A^\star})(u_A - u_{A^\star}), \quad v_{\mathcal{T}}, u_{\mathcal{T}} \in \mathbb{R}^{\mathcal{T}}. \tag{2.5}$$

In particular, when $v_{\mathcal{T}} = u_{\mathcal{T}}$ one gets

$$\left[\!\left[\mathcal{P}^{\mathcal{T}} v_{\mathcal{T}}, v_{\mathcal{T}}\right]\!\right]_{\mathcal{T}} = \frac{1}{2}\frac{1}{h^\eta}\sum_{A \in \mathfrak{M}}\sum_{A^\star \in \overline{\mathfrak{M}^\star}} |A \cap A^\star|\,(v_A - v_{A^\star})^2 = \frac{1}{2}\frac{1}{h^\eta}\left\|v_{\mathfrak{M}} - v_{\overline{\mathfrak{M}^\star}}\right\|^2_{L^2(\Omega)}. \tag{2.6}$$

The considered problem is time-dependent. Then, the discretization of the time interval $(0, t_f)$ is given by an increasing finite sequence of instants $t^0 = 0 < t^1 < \cdots < t^N = t_f$. This subdivision is assumed to be uniform with a time step δt. Thereby, $t^n = n\delta t$. Let us take a family of vectors $(v_{\mathcal{T}}^n)_{n=0,\cdots N}$ of $\mathbb{R}^{\mathcal{T}}$. We define the discrete reconstructions in time $v_{\mathfrak{M},\delta t}$ and $v_{\overline{\mathfrak{M}^\star},\delta t}$ such that

$$v_{\mathfrak{M},\delta t}(x,t) = v_A^n \quad \forall (x,t) \in A \times (t^{n-1}, t^n],\ \forall A \in \mathfrak{M},\ \forall n \geq 1,$$
$$v_{\overline{\mathfrak{M}^\star},\delta t}(x,t) = v_{A^\star}^n \quad \forall (x,t) \in A^\star \times (t^{n-1}, t^n],\ \forall A^\star \in \overline{\mathfrak{M}^\star},\ \forall n \geq 1.$$

We also denote

$$v_{h,\delta t} = \frac{1}{2}\Big(v_{\mathfrak{M},\delta t} + v_{\overline{\mathfrak{M}^\star},\delta t}\Big).$$

Similarly, we define the reconstruction of the discrete gradient in time by

$$\nabla_{\mathfrak{S},\delta t} v_{\mathcal{T}}(x,t) = \nabla_{\mathcal{D}} v_{\mathcal{T}}^n \quad \forall (x,t) \in \mathcal{D} \times (t^{n-1}, t^n],\ \forall \mathcal{D} \in \mathfrak{S},\ \forall n \geq 1.$$

The tensor Λ is approximated using the following mean

$$\Lambda_{\mathfrak{S}}(x) := \Lambda^{\mathcal{D}} = \frac{1}{|\mathcal{D}|}\int_{\mathcal{D}} \Lambda(s)\,\mathrm{d}s \quad \forall x \in \mathcal{D},\ \forall \mathcal{D} \in \mathfrak{S}.$$

Notice that $\Lambda^{\mathcal{D}}$ is still positive-definite for all $\mathcal{D}$.

2.2 Generic finite volume scheme

Let us here provide a generic finite volume discretization of the diffusive part in (1.5). A finite volume scheme is usually generated from a set of discrete conservative fluxes. Let $K \in \mathfrak{M} \cup \overline{\mathfrak{M}^\star}$ be a control volume of interest which is characterized by its mass center x_K, set of edges $\mathcal{E}_K$ and the corresponding unit normal vectors $\{\mathbf{n}_{\nu,K}\}_{\nu\in\mathcal{E}_K}$ to these interfaces outwards K. We omit the time-dependency for the moment. The first step consists in integrating the diffusion term over K. Applying Green's formula, one gets the balance equation

$$-\int_K \operatorname{div} \beta(p)\Lambda\nabla\beta(p)\,\mathrm{d}x = -\sum_{\nu\in\mathcal{E}_K}\int_\nu \beta(p)\Lambda\nabla\beta(p)\cdot\mathbf{n}_{\nu,K}\,\mathrm{d}S(x).$$

We then propose the following natural approximation of the continuous flux

$$-\int_\nu \beta(p)\Lambda\nabla\beta(p)\cdot\mathbf{n}_\nu\,\mathrm{d}S(x) \approx \beta(p_\nu)F_{K,\nu}(\beta(p_\mathcal{T})). \tag{2.7}$$

Let us select a cell L in the same finite volume partition as K such that it shares the interface ν i.e. $\nu = K|L \in \mathcal{E}_K \cap \mathcal{E}_L$. The key expression of the coefficient $\beta(p_{K|L}) = \beta(p_\nu)$ is given by the centered formula

$$\beta(p_{K|L}) = \begin{cases} \dfrac{\beta(p_K)-\beta(p_L)}{\log(\beta(p_K))-\log(\beta(p_L))} & \text{if } \beta(p_K)\neq\beta(p_L) \\ \\ \beta(p_K) & \text{else} \end{cases}. \tag{2.8}$$

A variant of this expression of $\beta(p_{K|L})$ has been introduced in [11] to preserve the equilibrium. It has also played an intermediary role in the convergence analysis of the numerical scheme proposed in [20]. We have recently established in [44] that such a choice is more stable and robust than the arithmetic average for the linear diffusion equation with a drift. Contrary to well-known means, like the arithmetic mean or the harmonic one, in the theory of finite volume methods, we will see that the crucial average (2.8) is of great importance for the analysis. Particularly, it will allow to derive some uniform estimations in a straightforward way. It is also used to maintain the optimal numerical accuracy of the discrete fluxes and that of the approximate solution. More importantly, the function $F_{K,\nu}(\beta(p_\mathcal{T}))$ is obtained by substituting the continuous gradient by its discrete counterpart on the diamond cell formed around the interface ν. Then, one writes

$$F_{K,\nu}(\beta(p_\mathcal{T})) = |\nu|\,\Lambda^{\mathcal{D}_\nu}\nabla_{\mathcal{D}_\nu}\beta(p_\mathcal{T})\cdot\mathbf{n}_{\nu,K}. \tag{2.9}$$

The discrete flux given in (2.7) satisfies the local conservation property

$$\beta(p_\nu)F_{K,\nu}(\beta(p_\mathcal{T})) = -\beta(p_\nu)F_{L,\nu}(\beta(p_\mathcal{T})), \quad \forall \nu = K|L \in \mathcal{E}_K\cap\mathcal{E}_L.$$

Note that the above discretization could be extended to a multi-dimensional abstract framework as far as one provides an appropriate consistent (weak or strong) approximation of the gradient operator. For instance, it can applied to the standard schemes written in the two-point formalism like TPFA [31], conforming CVFE methods [2, 19, 45] as well as the multi-point framework such as VAG [34, 15, 20], HMM [17, 28] approaches. For more details on how these methods accord with our setting, the reader can consult their constructions in this review [27].

Remark 2.1. *Another possible option to choose $\beta(p_\nu)$ in (2.7) is to consider the following upwind scheme [45]*

$$\beta(p_{K|L}) = \begin{cases} \beta(p_K) & \text{if } F_{K,\nu}(\beta(p_\mathcal{T}))\geq 0 \\ \beta(p_L) & \text{if } F_{K,\nu}(\beta(p_\mathcal{T}))<0 \end{cases}.$$

We hereafter will not take into account this kind of approximation since it only yields first order accuracy in space. It is however conservative and consistent. It moreover allows to obtain the cornerstone a priori estimations as we will see later on. Therefore the analysis carried out throughout this work is still valid.

2.3 Discrete conservation equations

In this work, we use the nonlinear DDFV method in space and the (backward) Euler implicit scheme in time to discretize the parabolic problem (1.1)-(1.3). The approximation of the fluxes stems from the framework (2.7)-(2.9).

The discretization of the initial state of the solution is commonly given by the means

$$p_K^0 = \frac{1}{|K|}\int_K p^0(x)\,\mathrm{d}x, \quad \forall K \in \mathfrak{M} \cup \overline{\mathfrak{M}^\star}, \quad p_A^0 = 0, \quad \forall A \in \partial\mathfrak{M}. \tag{2.10}$$

For $1 \leq n \leq N$, we compute $p_{\mathcal{T}}^n \in (\mathbb{R}_{+,*})^{\mathcal{T}}$ satisfying the discrete conservation equations

$$\frac{|A|}{\delta t}(p_A^n - p_A^{n-1}) + \sum_{\mathcal{D}_{\sigma,\sigma^\star}\in\mathcal{D}_A} \beta(p_\sigma^n)F_{A,\sigma}(\beta(p_{\mathcal{T}}^n)) + \lambda\,|A|\,\mathcal{P}_A^{\mathcal{T}}\log\left(\beta(p_{\mathcal{T}}^n)\right) = 0, \quad \forall A \in \mathfrak{M}, \tag{2.11}$$

$$\frac{|A^\star|}{\delta t}(p_{A^\star}^n - p_{A^\star}^{n-1}) + \sum_{\mathcal{D}_{\sigma,\sigma^\star}\in\mathcal{D}_{A^\star}} \beta(p_{\sigma^\star}^n)F_{A^\star,\sigma^\star}(\beta(p_{\mathcal{T}}^n)) + \lambda\,|A^\star|\,\mathcal{P}_{A^\star}^{\mathcal{T}}\log\left(\beta(p_{\mathcal{T}}^n)\right) = 0, \quad \forall A^\star \in \overline{\mathfrak{M}^\star}. \tag{2.12}$$

The fixed parameter λ serves to stabilize the scheme. In the case where $A \in \partial\mathfrak{M}$, the value p_A^n is determined by considering the equation

$$F_{A,\sigma}(\beta(p_{\mathcal{T}}^n)) = |\sigma|\,\Lambda^{\mathcal{D}_\nu}\nabla_{\mathcal{D}}\beta(p_{\mathcal{T}}^n)\cdot\mathbf{n}_{\sigma,A} = 0, \qquad \text{with } \mathcal{D} = \mathcal{D}_{\sigma,\sigma^\star} \in \mathfrak{S}_{\mathrm{ext}}. \tag{2.13}$$

Notice that if the solution to the above numerical scheme exists, it is necessarily positive. In the sequel, we will utilize the following identity frequently

$$\begin{aligned}\frac{1}{\delta t}\left[\!\left[p_{\mathcal{T}}^n - p_{\mathcal{T}}^{n-1}, u_{\mathcal{T}}\right]\!\right]_{\mathcal{T}} + \frac{1}{2}\sum_{\mathcal{D}_{\sigma,\sigma^\star}\in\mathfrak{S}} &\beta(p_\sigma^n)F_{A,\sigma}(\beta(p_{\mathcal{T}}^n))(u_A - u_B) + \beta(p_{\sigma^\star}^n)F_{A^\star,\sigma^\star}(\beta(p_{\mathcal{T}}^n))(u_{A^\star} - u_{B^\star}) \\ &+ \lambda\left[\!\left[\mathcal{P}^{\mathcal{T}}\log\left(\beta(p_{\mathcal{T}}^n)\right), u_{\mathcal{T}}\right]\!\right]_{\mathcal{T}} = 0, \quad \forall u_{\mathcal{T}} \in \mathbb{R}^{\mathcal{T}}.\end{aligned} \tag{2.14}$$

We will sometimes write (by abuse of notation) $\mathcal{D} = \mathcal{D}_{\sigma,\sigma^\star}$ with $\sigma = A|B$ and $\sigma^\star = A^\star|B^\star$. The above result is obtained after a couple of manipulations on the scheme. First, we multiply (2.11) (resp.(2.12)) by u_A (resp. $u_{A^\star}$) and sum on all the primal (resp. dual) cells. We then introduce the local conservation of the fluxes to rearrange each summation by edges. Finally, we add together the resulting equations so that one ends up with (2.14).

Let us next study some mathematical properties fulfilled by the above numerical scheme, namely the a priori estimates that are exploited in particular to establish the existence of a solution to the nonlinear system (2.10)-(2.13).

3 A priori estimates and existence of discrete solutions

In this section, we first claim the conservation of mass and take advantage of the crucial relationships $(2.7)-(2.9)$ to derive a uniform estimate on the discrete gradient of $\beta(p_{\mathcal{T}}^n)$ as well as the entropy function $\Upsilon(p_{\mathcal{T}}^n)$. Having these properties in hand will allow us to perform the analysis of the proposed scheme. Unless specified, we denote by C a generic constant that depends only on the data and on the mesh regularity.

Proposition 3.1. *Consider $p_{\mathcal{T}}^n \in (\mathbb{R}_{+,*})^{\mathcal{T}}$ a solution to the scheme (2.10)-(2.13) for all $n \geq 1$. Then, the mass is conserved at each time level i.e.*

$$\int_\Omega p_h^n(x)\,\mathrm{d}x = \int_\Omega p^0(x)\,\mathrm{d}x, \quad \forall n \geq 1. \tag{3.1}$$

Moreover, there exists $C > 0$ depending only on the data such that the inequality below holds true

$$\|\nabla_{\mathfrak{S},\delta t}\beta(p_{\mathcal{T}})\|_{L^2(Q_{t_f})^2}^2 + \lambda\sum_{n=1}^N \delta t\left[\!\left[\mathcal{P}^{\mathcal{T}}\log\left(\beta(p_{\mathcal{T}}^n)\right), \log(\beta(p_{\mathcal{T}}^n))\right]\!\right]_{\mathcal{T}} \leq C. \tag{3.2}$$

Consequently

$$\sum_{n=1}^{N} \delta t \sum_{\mathcal{D}\in\mathfrak{S}} |\delta_{\mathcal{D}}\beta(p_{\mathcal{T}}^n)|^2 \leq C. \tag{3.3}$$

The entropy function is uniformly bounded in the sense

$$\|\Upsilon(p_{h,\delta t})\|_{L^\infty(0,t_f;L^1(\Omega))} \leq C. \tag{3.4}$$

Furthermore, one has

$$\|\beta(p_{\mathfrak{M},\delta t})\|_{L^2(Q_{t_f})} \leq C \quad \text{and} \quad \left\|\beta(p_{\overline{\mathfrak{M}^\star},\delta t})\right\|_{L^2(Q_{t_f})} \leq C. \tag{3.5}$$

Proof. Taking all the components of $u_{\mathcal{T}}$ to be 1 in (2.14) entails the first point (3.1) directly. Let us prove the second one. Let us again select $u_{\mathcal{T}} = \log(\beta(p_{\mathcal{T}}^n))$ in the same relationship (2.14) and sum over $n \geq 1$ to get

$$X_1 + X_2 + X_3 = 0, \tag{3.6}$$

where

$$\begin{aligned}
X_1 &= \sum_{n=1}^{N} \left[\!\left[p_{\mathcal{T}}^n - p_{\mathcal{T}}^{n-1}, \log(\beta(p_{\mathcal{T}}^n)) \right]\!\right]_{\mathcal{T}}, \\
X_2 &= \frac{1}{2} \sum_{n=1}^{N} \delta t \sum_{\mathcal{D}\in\mathfrak{S}} \beta(p_\sigma^n) F_{A,\sigma}(\beta(p_{\mathcal{T}}^n)) \Big(\log(\beta(p_A^n)) - \log(\beta(p_B^n)) \Big) \\
&\qquad + \beta(p_{\sigma^\star}^n) F_{A^\star,\sigma^\star}(\beta(p_{\mathcal{T}}^n)) \Big(\log(\beta(p_{A^\star}^n)) - \log(\beta(p_{B^\star}^n)) \Big), \\
X_3 &= \lambda \sum_{n=1}^{N} \delta t \left[\!\left[\mathcal{P}^{\mathcal{T}} \log\left(\beta(p_{\mathcal{T}}^n)\right), \log(\beta(p_{\mathcal{T}}^n)) \right]\!\right]_{\mathcal{T}}.
\end{aligned}$$

Using the convexity of the entropy function Υ, it can be checked that

$$\begin{aligned}
X_1 &\geq \sum_{n=1}^{N} \left[\!\left[\Upsilon(p_{\mathcal{T}}^n) - \Upsilon(p_{\mathcal{T}}^{n-1}), \mathbf{1}_{\mathcal{T}} \right]\!\right]_{\mathcal{T}} = \left[\!\left[\Upsilon(p_{\mathcal{T}}^N) - \Upsilon(p_{\mathcal{T}}^0), \mathbf{1}_{\mathcal{T}} \right]\!\right]_{\mathcal{T}} \\
&\geq - \left[\!\left[\Upsilon(p_{\mathcal{T}}^0), \mathbf{1}_{\mathcal{T}} \right]\!\right]_{\mathcal{T}} \geq - \left\| \Upsilon(p^0) \right\|_{L^1(\Omega)},
\end{aligned} \tag{3.7}$$

thanks to Jensen's inequality. The key formulas (2.8)-(2.9) assert

$$\begin{aligned}
&\beta(p_\sigma^n) F_{A,\sigma}(\beta(p_{\mathcal{T}}^n)) \Big(\log(\beta(p_A^n)) - \log(\beta(p_B^n)) \Big) = |\sigma|\, \Lambda^{\mathcal{D}} \nabla_{\mathcal{D}} \beta(p_{\mathcal{T}}^n) \cdot \Big(\beta(p_A^n) - \beta(p_B^n) \Big) \mathbf{n}_{\sigma,A}, \\
&\beta(p_{\sigma^\star}^n) F_{A^\star,\sigma^\star}(\beta(p_{\mathcal{T}}^n)) \Big(\log(\beta(p_{A^\star}^n)) - \log(\beta(p_{B^\star}^n)) \Big) = |\sigma^\star|\, \Lambda^{\mathcal{D}} \nabla_{\mathcal{D}} \beta(p_{\mathcal{T}}^n) \cdot \Big(\beta(p_{A^\star}^n) - \beta(p_{B^\star}^n) \Big) \mathbf{n}_{\sigma^\star,A^\star}.
\end{aligned}$$

As consequence of these identities, the expression of the discrete gradient and Assumption **(ii)**, one gets

$$\begin{aligned}
X_2 &= \sum_{n=1}^{N} \delta t \sum_{\mathcal{D}\in\mathfrak{S}} |\mathcal{D}|\, \Lambda^{\mathcal{D}} \nabla_{\mathcal{D}} \beta(p_{\mathcal{T}}^n) \cdot \nabla_{\mathcal{D}} \beta(p_{\mathcal{T}}^n) \\
&\geq \underline{\Lambda} \sum_{n=1}^{N} \delta t \, \|\nabla_{\mathfrak{S}} \beta(p_{\mathcal{T}}^n)\|_{L^2(\Omega)^2}^2.
\end{aligned} \tag{3.8}$$

We collect (3.6)-(3.8) to deduce (3.2) with $C = (1 + \frac{1}{\underline{\Lambda}}) \left\| \Upsilon(p^0) \right\|_{L^1(\Omega)}$. Mimicking similar steps one refinds that

$$\begin{aligned}
&\left[\!\left[\Upsilon(p_{\mathcal{T}}^n) - \Upsilon(p_{\mathcal{T}}^{n-1}), \mathbf{1}_{\mathcal{T}} \right]\!\right]_{\mathcal{T}} + \delta t \sum_{\mathcal{D}\in\mathfrak{S}} |\mathcal{D}|\, \Lambda^{\mathcal{D}} \nabla_{\mathcal{D}} \beta(p_{\mathcal{T}}^n) \cdot \nabla_{\mathcal{D}} \beta(p_{\mathcal{T}}^n) \\
&\qquad + \lambda \delta t \left[\!\left[\mathcal{P}^{\mathcal{T}} \log\left(\beta(p_{\mathcal{T}}^n)\right), \log(\beta(p_{\mathcal{T}}^n)) \right]\!\right]_{\mathcal{T}} \leq 0, \quad \forall n \geq 1.
\end{aligned}$$

Using (2.6) we see that the third term in the previous inequality is nonnegative. The nonnegativity of the diffusion part forces

$$0 \leq [\![\Upsilon(p_{\mathcal{T}}^n), \mathbf{1}_{\mathcal{T}}]\!]_{\mathcal{T}} \leq [\![\Upsilon(p_{\mathcal{T}}^{n-1}), \mathbf{1}_{\mathcal{T}}]\!]_{\mathcal{T}} \leq \cdots \leq \left\|\Upsilon(p^0)\right\|_{L^1(\Omega)}, \quad \forall n \geq 1.$$

As a result

$$\|\Upsilon(p_{h,\delta t})\|_{L^\infty(0,t_f;L^1(\Omega))} \leq \left\|\Upsilon(p^0)\right\|_{L^1(\Omega)}.$$

Let us finally show the last two inequalities. Following [20] and owing to assumption (1.7) one has : for all $0 < \varepsilon \leq 1$ there exists r_ε such that

$$\beta(s)^2 \leq \epsilon \Upsilon(s), \quad \forall s > r_\varepsilon.$$

Since β^2 is a continuous function, its maximum on $[0, r_\varepsilon]$ exists and is finite. We denote it by $C_{\beta,\varepsilon}$. We take $\varepsilon = 1$. Then, one gets

$$\beta(s)^2 \leq C_{\beta,1} + \Upsilon(s), \quad \forall s \geq 0.$$

As a consequence of this and (3.4), we find

$$\sum_{n=1}^{N} \delta t \sum_{A \in \mathfrak{M}} |A| \, \beta(p_A^n)^2 \leq t_f C_{\beta,1} \, |\Omega| + \sum_{n=1}^{N} \delta t \sum_{A \in \mathfrak{M}} |A| \, \Upsilon(p_A^n) \leq t_f C_{\beta,1} \, |\Omega| + 2 t_f \left\|\Upsilon(p^0)\right\|_{L^1(\Omega)}.$$

Therefore, one obtains

$$\|\beta(p_{\mathfrak{M},\delta t})\|_{L^2(Q_{t_f})} \leq C.$$

Similarly, we establish the L^2 norm on $\beta(p_{\overline{\mathfrak{M}^\star},\delta t})$. □

Let us denote $\widehat{\beta}_{\mathfrak{S},\delta t}, \widehat{\beta}^\star_{\mathfrak{S},\delta t}$ two piecewise constant functions on the diamond cells defined as follows

$$\widehat{\beta}_{\mathfrak{S},\delta t}(x,t) = \beta(p_\sigma^n), \text{ and } \widehat{\beta}^\star_{\mathfrak{S},\delta t}(x,t) = \beta(p_{\sigma^\star}^n), \quad \forall (x,t) \in \mathcal{D} \times (t^{n-1}, t^n], \quad \forall \mathcal{D} \in \mathfrak{S}, \forall n \geq 1.$$

We show in the following result that these functions are bounded in $L^2(Q_{t_f})$ independently of the meshes.

Corollary 3.1. *There exists C independent of the mesh size and the time step such that*

$$\left\|\widehat{\beta}_{\mathfrak{S},\delta t} - \beta(p_{\mathfrak{M},\delta t})\right\|_{L^2(Q_{t_f})} \leq Ch, \text{ and } \left\|\widehat{\beta}^\star_{\mathfrak{S},\delta t} - \beta(p_{\overline{\mathfrak{M}^\star},\delta t})\right\|_{L^2(Q_{t_f})} \leq Ch. \tag{3.9}$$

In particular, there holds

$$\left\|\widehat{\beta}_{\mathfrak{S},\delta t}\right\|_{L^2(Q_{t_f})} \leq C, \qquad \left\|\widehat{\beta}^\star_{\mathfrak{S},\delta t}\right\|_{L^2(Q_{t_f})} \leq C. \tag{3.10}$$

Proof. By construction, we observe that the function $\widehat{\beta}_{\mathfrak{S},\delta t}$ fulfills

$$\min\left(\beta(p_A^n), \beta(p_B^n)\right) \leq \beta(p_\sigma^n) \leq \max\left(\beta(p_A^n), \beta(p_B^n)\right),$$

for all $\mathcal{D}_{\sigma,\sigma^\star} \in \mathfrak{S}$ with $\sigma = A|B$. Summing on the diamond cells and making use of (3.3) lead to

$$\left\|\widehat{\beta}_{\mathfrak{S},\delta t} - \beta(p_{\mathfrak{M},\delta t})\right\|^2_{L^2(Q_{t_f})} \leq \sum_{n=1}^{N} \delta t \sum_{\mathcal{D} \in \mathfrak{S}} |\mathcal{D}| \, |\beta(p_A^n) - \beta(p_B^n)|^2 \leq h^2 \sum_{n=1}^{N} \delta t \sum_{\mathcal{D} \in \mathfrak{S}} |\delta_{\mathcal{D}} \beta(p_{\mathcal{T}}^n)|^2 \leq Ch^2.$$

Analogously, we prove the second inequality on the dual mesh. Taking advantage of (3.9) together with (3.5), one obtains the uniform bounds of (3.10). □

Remark 3.1. *The estimations of Proposition 3.1 is still valid if we consider the upwind scheme claimed in Remark 2.1. Let us show for instance how to obtain the first term of inequality* (3.2)*. We first mimic the same steps of the above proof. Then, by virtue of Remark 1.1, it suffices to write the upwind choice equivalently as follows*

$$\beta(p_\sigma^n) = \begin{cases} \max\limits_{I_{AB}^n} \beta(p) & \text{if } F_{A,\sigma}(\beta(p_{\mathcal{T}}^n))\Big(\beta(p_A^n) - \beta(p_B^n)\Big) \geq 0 \\ \min\limits_{I_{AB}^n} \beta(p) & \text{otherwise} \end{cases},$$

where $I_{AB}^n = [\min(p_A^n, p_B^n), \max(p_A^n, p_B^n)]$*. As a consequence, one gets*

$$\beta(p_\sigma^n) F_{A,\sigma}(\beta(p_{\mathcal{T}}^n))\Big(\log(\beta(p_A^n)) - \log(\beta(p_B^n))\Big) \geq |\sigma|\, \Lambda^{\mathcal{D}} \nabla_{\mathcal{D}} \beta(p_{\mathcal{T}}^n) \cdot \Big(\beta(p_A^n) - \beta(p_B^n)\Big)\mathbf{n}_{\sigma,A}.$$

An analogous idea can be applied to σ^**. With that, one ensures the validity of* (3.8) *in the case where the upstream method is taken into account.*

The next result shows a mesh-dependent lower bound on any solution to the discretized problem. The idea of the proof extends the argument provided in [18].

Proposition 3.2. *Let* $p_{\mathcal{T}}^n \in (\mathbb{R}_{+,*})^{\mathcal{T}}$ *be a solution to the coupled scheme* (2.10)-(2.13) *for all* $n \geq 1$*. Then, there exists a positive constant* $C_{h,\delta t}$ *that depends on the data and on the discretization steps such that*

$$p_h^n \geq C_{h,\delta t} > 0, \quad \forall n \geq 1. \tag{3.11}$$

Proof. The mass conservation (3.1) and Assumption **(iii)**-(a) ensures the existence of an $A_0 \in \mathfrak{M}$ that satisfies

$$p_{A_0}^n \geq \frac{1}{|\Omega|} \int_\Omega p^0(x)\, \mathrm{d}x > 0.$$

Therefore

$$\log(\beta(p_{A_0}^n)) \geq -C'.$$

Thanks to the uniform bound (3.2) on the penalization contribution together with the identity (2.6) we get

$$\delta t \frac{1}{2} \frac{1}{h^\eta} \sum_{A \in \mathfrak{M}} \sum_{A^\star \in \overline{\mathfrak{M}^\star}} |A \cap A^\star| \left(\log(\beta(p_A^n) - \log(\beta(p_{A^\star}^n))\right)^2 \leq C. \tag{3.12}$$

For each vertex (dual volume) $A_0^\star$ of A_0 we estimate

$$\Big|\log(\beta(p_{A_0}^n) - \log(\beta(p_{A_0^\star}^n))\Big| \leq C_{h,\delta t}^{0,0}.$$

Accordingly

$$\log(\beta(p_{A_0^\star}^n)) \geq -C_{h,\delta t}^{\star,0}.$$

We now apply the same procedure on the vertices of $A_0^\star$ except A_0. Such a primal cell is denoted by A_1. In its turn, it satisfies

$$\Big|\log(\beta(p_{A_1}^n) - \log(\beta(p_{A_0^\star}^n))\Big| \leq C_{h,\delta t}^{1,0}.$$

Consequently

$$\log(\beta(p_{A_1}^n)) \geq -C_{h,\delta t}^{1}.$$

Being inspired by [20], we continue in the described fashion by induction using always (3.12). We iterate once on the primal mesh and another on the dual mesh until we cover all the (primal and dual) cells . As a consequence we obtain

$$\log(\beta(p_K^n)) \geq -C''_{h,\delta t}, \quad \forall K \in \overline{\mathfrak{M}^\star} \cup \mathfrak{M}.$$

Furthermore, we know that β^{-1} exists, is continuous and is strictly increasing on $[0, \lim_{p \to +\infty} \beta(p))$. We finally deduce

$$p_K^n \geq \beta^{-1}\Big(e^{-C''_{h,\delta t}}\Big) > 0, \quad \forall K \in \overline{\mathfrak{M}^\star} \cup \mathfrak{M}.$$

This concludes the proof of (3.11). □

In the remainder of this section, we state without proof that the numerical scheme possesses at least one solution. The proof is an adaptation of the one given in [19] or in [20].

Proposition 3.3. *There exists a solution $p_{\mathcal{T}}^n \in (\mathbb{R}_{+,*})^{\mathcal{T}}$ to the nonlinear system (2.10)-(2.13) for all $n \geq 1$.*

4 Convergence towards the weak solution

The control of a dual norm on the discrete counterpart of the time derivative is of great help to establish that the sequence of solutions to the numerical scheme is relatively compact. Let φ be in $\mathcal{C}_c^\infty(\Omega)$. We associate the vector $\varphi_{\mathcal{T}}$ of $\mathbb{R}^{\mathcal{T}}$ defined per components as follows

$$\varphi_K = \frac{1}{|K|}\int_K \varphi(x)\,\mathrm{d}x, \quad \forall K \in \mathfrak{M} \cup \overline{\mathfrak{M}^\star}, \text{ and } \varphi_K = 0, \quad \forall K \in \partial\mathfrak{M}.$$

Lemma 4.1. *There exists a constant C independent of the discretization parameters such that*

$$\sum_{n=1}^{N} \left[\!\left[p_{\mathcal{T}}^n - p_{\mathcal{T}}^{n-1}, \varphi_{\mathcal{T}} \right]\!\right]_{\mathcal{T}} \leq C \left\|\nabla\varphi\right\|_{L^\infty(\Omega)}, \quad \forall \varphi \in \mathcal{C}_c^\infty(\Omega).$$

Proof. We take $u_{\mathcal{T}} = \varphi_{\mathcal{T}}$ in the relationship (2.14) and split its left hand side into three parts as follows

$$\mathcal{Z}_1 + \mathcal{Z}_2 + \mathcal{Z}_3 = 0, \tag{4.1}$$

where each term after summing on all $n \geq 1$ reads

$$\mathcal{Z}_1 = \sum_{n=1}^{N} \left[\!\left[p_{\mathcal{T}}^n - p_{\mathcal{T}}^{n-1}, \varphi_{\mathcal{T}} \right]\!\right]_{\mathcal{T}},$$

$$\mathcal{Z}_2 = \frac{1}{2}\sum_{n=1}^{N} \delta t \sum_{\mathcal{D}_{\sigma,\sigma^\star}\in\mathfrak{S}} \beta(p_\sigma^n) F_{A,\sigma}(\beta(p_{\mathcal{T}}^n))(\varphi_A - \varphi_B) + \beta(p_{\sigma^\star}^n) F_{A^\star,\sigma^\star}(\beta(p_{\mathcal{T}}^n))(\varphi_{A^\star} - \varphi_{B^\star}),$$

$$\mathcal{Z}_3 = \lambda \sum_{n=1}^{N} \delta t \left[\!\left[\mathcal{P}^{\mathcal{T}} \log\left(\beta(p_{\mathcal{T}}^n)\right), \varphi_{\mathcal{T}} \right]\!\right]_{\mathcal{T}}.$$

Let us estimate the diffusion contribution. First, we combine the fact that $\Lambda^{\mathcal{D}}$ is positive-definite and uniformly coercive together with the Cauchy-Schwarz inequality to see that

$$|F_{A,\sigma}(\beta(p_{\mathcal{T}}^n))| \leq |\sigma| \left(\Lambda^{\mathcal{D}} \nabla_{\mathcal{D}}\beta(p_{\mathcal{T}}^n) \cdot \nabla_{\mathcal{D}}\beta(p_{\mathcal{T}}^n)\right)^{\frac{1}{2}} \left(\Lambda^{\mathcal{D}}\mathbf{n}_{\sigma,A}\cdot\mathbf{n}_{\sigma,A}\right)^{\frac{1}{2}} \leq \overline{\Lambda}\,|\sigma|\,|\nabla_{\mathcal{D}}\beta(p_{\mathcal{T}}^n)|.$$

A similar result holds in the case of a dual interface. Additionally, since φ is smooth there exists a constant C depending only on the mesh regularity such that

$$|\varphi_A - \varphi_B| \leq C\,|\sigma^*|\,\|\nabla\varphi\|_{L^\infty(\Omega)} \text{ and } |\varphi_{A^\star} - \varphi_{B^\star}| \leq C\,|\sigma|\,\|\nabla\varphi\|_{L^\infty(\Omega)}.$$

As a consequence, one gets

$$\begin{aligned}
|\mathcal{Z}_2| &\leq \frac{1}{2}\overline{\Lambda}\,\|\nabla\varphi\|_{L^\infty(\Omega)}\, C \sum_{n=1}^{N} \delta t \sum_{\mathcal{D}_{\sigma,\sigma^\star}\in\mathfrak{S}} |\mathcal{D}|\left(\beta(p_\sigma^n) + \beta(p_{\sigma^\star}^n)\right)|\nabla_{\mathcal{D}}\beta(p_{\mathcal{T}}^n)| \\
&\leq C\,\|\nabla\varphi\|_{L^\infty(\Omega)} \left(\left\|\widehat{\beta}_{\mathfrak{S},\delta t}\right\|_{L^2(Q_{t_f})} + \left\|\widehat{\beta}^\star_{\mathfrak{S},\delta t}\right\|_{L^2(Q_{t_f})}\right) \|\nabla_{\mathfrak{S},\delta t}\beta(p_{\mathcal{T}}^n)\|_{L^2(Q_{t_f})^2} \\
&\leq C\,\|\nabla\varphi\|_{L^\infty(\Omega)}.
\end{aligned} \tag{4.2}$$

The latter inequality holds thanks to (3.2) and (3.10). Next, we treat the penalty part. Owing to (2.5) and the Cauchy-Schwarz inequality we claim

$$|\mathcal{Z}_3| \leq \lambda t_f^{\frac{1}{2}} \left(\sum_{n=1}^{N} \delta t \left[\!\left[\mathcal{P}^{\mathcal{T}} \log\left(\beta(p_{\mathcal{T}}^n)\right), \log(\beta(p_{\mathcal{T}}^n)) \right]\!\right]_{\mathcal{T}}\right)^{\frac{1}{2}} \left[\!\left[\mathcal{P}^{\mathcal{T}}\varphi_{\mathcal{T}}, \varphi_{\mathcal{T}} \right]\!\right]_{\mathcal{T}}^{\frac{1}{2}}.$$

The regularity of φ implies

$$[\![\mathcal{P}^{\mathcal{T}}\varphi_{\mathcal{T}},\varphi_{\mathcal{T}}]\!]_{\mathcal{T}}^{\frac{1}{2}} = \frac{1}{\sqrt{2}}\frac{1}{h^{\eta/2}}\left\|\varphi_{\mathfrak{M}} - \varphi_{\overline{\mathfrak{M}^\star}}\right\|_{L^2(\Omega)} \leq Ch^{1-(\eta/2)}\left\|\nabla\varphi\right\|_{L^\infty(\Omega)} \leq C\left\|\nabla\varphi\right\|_{L^\infty(\Omega)},$$

where again C depends only on the mesh regularity, λ, η and Ω. Applying once more (3.2) yields $|\mathcal{Z}_3| \leq C\left\|\nabla\varphi\right\|_{L^\infty(\Omega)}$. □

Theorem 4.1. *Let $(\mathcal{T}_k)_{k\in\mathbb{N}}$ be a sequence of DDFV discretizations to Ω and $(\delta t_k)_{k\in\mathbb{N}}$ a sequence of time steps such that h_k and δt_k go to 0 as $k\to+\infty$. There exists a weak solution p to (1.1)-(1.3) in the sense of Definition 1.1 such that*

$$p_{\mathfrak{M}_k,\delta t_k}, p_{\overline{\mathfrak{M}^\star}_k,\delta t_k}, p_{h_k,\delta t_k} \longrightarrow p \qquad \text{a.e. in } Q_{t_f}, \text{ and strongly in } L^1(Q_{t_f}), \tag{4.3}$$

$$\nabla_{\mathfrak{S}_k,\delta t_k}\beta(p_{\mathcal{T}_k}) \longrightarrow \nabla\beta(p) \qquad \text{weakly in } L^2(Q_{t_f})^2, \tag{4.4}$$

$$\beta(p_{\mathfrak{M}_k,\delta t_k}), \beta(p_{\overline{\mathfrak{M}^\star}_k,\delta t_k}), \beta(p_{h_k,\delta t_k}) \longrightarrow \beta(p) \qquad \text{strongly in } L^2(Q_{t_f}), \tag{4.5}$$

up to a subsequence as $k\to+\infty$.

Proof. In this proof, we propose to apply the recent compactness criterion [8, Theorem 3.9] which is mainly dedicated to degenerate parabolic equations. The main elements, labeled $(\mathbf{A}_t)$, $(\mathbf{A}_x\mathbf{1})$, $(\mathbf{A}_x\mathbf{2})$ and $(\mathbf{A}_x\mathbf{3})$ in [7], to make use of this result are checked in our context and summarized in the following list.

(a) We consider a one-step discretization in time. As a consequence, the item $(\mathbf{A}_t)$ always holds true.

(b) Following the arguments developed in [7] one can show, using a discrete Poincaré-Sobolev embedding [12], that any sequence $u_{\mathcal{T}_k} \in \mathbb{R}^{\mathcal{T}_k}$ satisfying

$$\|u_{h_k}\|_{L^2(\Omega)} + \|\nabla_{\mathfrak{S}_k} u_{\mathcal{T}_k}\|_{L^2(\Omega)^2} \leq C,$$

implies that $u_{\mathfrak{M}_k}$ and $u_{\overline{\mathfrak{M}^\star}_k}$ are relatively compact in $L^2(\Omega)$. Hence, the condition $(\mathbf{A}_x\mathbf{1})$ is fulfilled.

(c) The function $u_{\mathfrak{M}_k}$ (resp. $u_{\overline{\mathfrak{M}^\star}_k}$) is piecewise constant on the primal (resp. dual) cells. Then, the property $(\mathbf{A}_x\mathbf{2})$ holds also.

(d) Let ϕ be in $\mathcal{C}^\infty(\overline{\Omega})$ and consider $\phi_{\mathcal{T}_k} \in \mathbb{R}^{\mathcal{T}_k}$ such that

$$\phi_K = \frac{1}{|K|}\int_K \phi(x)\,\mathrm{d}x, \quad \forall K \in \mathfrak{M}_k \cup \overline{\mathfrak{M}^\star}_k, \text{ and } \phi_K = \frac{1}{|\sigma|}\int_\sigma \phi(x)\,\mathrm{d}x, \quad \forall K \equiv \sigma \in \partial\mathfrak{M}_k.$$

Following [22], the smoothness of ϕ entails

$$\|\phi_{h_k}\|_{L^\infty(\Omega)} + \|\nabla_{\mathfrak{S}_k}\phi_{\mathcal{T}_k}\|_{L^\infty(\Omega)} \leq C\left\|\nabla\phi\right\|_{L^\infty(\Omega)}.$$

where C is depending on the mesh regularity. This implies the validation of $(\mathbf{A}_x\mathbf{3})$.

Thanks to Lemma 4.1 we are now in a position to apply [8, Theorem 3.9]. It claims that there exist two possibly different measurable functions referred to as $p^{(1)}$ and $p^{(2)}$ such that one has up to a subsequence

$$p_{\mathfrak{M}_k,\delta t_k} \xrightarrow[k\to\infty]{} p^{(1)} \text{ and } p_{\overline{\mathfrak{M}^\star}_k,\delta t_k} \xrightarrow[k\to\infty]{} p^{(2)} \quad \text{a.e. in } Q_{t_f}. \tag{4.6}$$

The penalty contribution allows the identification of $p^{(1)}$ to $p^{(2)}$. Using (2.6) and the energy estimate (3.2) we hence check

$$\left\|\log\left(\beta(p_{\mathfrak{M}_k,\delta t_k})\right) - \log\left(\beta(p_{\overline{\mathfrak{M}^\star}_k,\delta t_k})\right)\right\|_{L^2(Q_{t_f})} \leq Ch_k^\eta \xrightarrow[k\to\infty]{} 0.$$

Extracting a new subsequence gives

$$\log\left(\beta(p_{\mathfrak{M}_k,\delta t_k})\right) - \log\left(\beta(p_{\overline{\mathfrak{M}^\star}_k,\delta t_k})\right) \xrightarrow[k\to\infty]{} 0 \quad \text{a.e. in } Q_{t_f}.$$

According to (4.6), there holds

$$\log\big(\beta(p_{\mathfrak{M}_k,\delta t_k})\big) \xrightarrow[k\to\infty]{} \log\big(\beta(p^{(1)})\big) \text{ and } \log\big(\beta(p_{\overline{\mathfrak{M}^\star}_k,\delta t})\big) \xrightarrow[k\to\infty]{} \log\big(\beta(p^{(2)})\big) \quad \text{a.e. in } Q_{t_f}.$$

Thereby $\log\big(\beta(p^{(1)})\big) = \log\big(\beta(p^{(2)})\big)$ a.e. in Q_{t_f}, yielding $p^{(1)} = p^{(2)}$ a.e. in Q_{t_f}, since β is invertible. Hereafter, this limit will be denoted by p. As a consequence

$$p_{h_k,\delta t_k}, p_{\overline{\mathfrak{M}^\star}_k,\delta t_k}, p_{h_k,\delta t_k} \xrightarrow[k\to\infty]{} p \quad \text{a.e. in } Q_{t_f}.$$

Additionally, Assumption **(iii)** states that the entropy function Υ is convex and increasing. It satisfies in particular that

$$\frac{\Upsilon(s)}{s} \longrightarrow +\infty \quad as \quad s \longrightarrow +\infty.$$

This condition and (3.4) allow us to apply De la Vallée Poussin criterion [13] for establishing the uniform integrability of the sequences $p_{\mathfrak{M}_k,\delta t_k}$ and $p_{\overline{\mathfrak{M}^\star}_k,\delta t_k}$. On the other hand, Vitali's convergence theorem guarantees that

$$p_{\mathfrak{M}_k,\delta t_k}, p_{\overline{\mathfrak{M}^\star}_k,\delta t_k} \longrightarrow p \quad \text{strongly in } L^1(Q_{t_f}).$$

The same result holds true for $p_{h_k,\delta t_k}$. Now, Proposition (3.1) and the a.e. convergence (4.3) claim the existence of Φ such that

$$\beta(p_{\mathcal{T}_k}) \longrightarrow \beta(p) \quad \text{weakly in } L^2(Q_{t_f}) \quad \text{and} \quad \nabla_{\mathfrak{S}_k,\delta t_k}\beta(p_{\mathcal{T}_k}) \longrightarrow \Phi \quad \text{weakly in } L^2(Q_{t_f})^2.$$

The identification of the limit process in the DDFV framework [7] entails $\Phi = \nabla\beta(p)$. To reinforce the strong convergence (4.5) we also have resort to Assumption **(iii)**, especially the condition

$$\frac{\Upsilon(s)}{\beta(s)^2} \longrightarrow +\infty \quad as \quad s \longrightarrow +\infty,$$

which enables us to reproduce a similar proof as done for (4.3), but this time in the L^2 norm. Indeed, De la Vallée Poussin property permits the uniform integrability of $\beta(p_{\mathfrak{M}_k,\delta t_k})^2$ and $\beta(p_{\overline{\mathfrak{M}^\star}_k,\delta t_k})^2$. Another application of Vitali's convergence theorem is then sufficient to conclude.

What is left is to check that p satisfies the weak formulation described in Definition 1.1. To begin with, let ψ be a test function in $\mathcal{C}_c^\infty(\overline{\Omega}\times[0,t_f))$. For all $n\geq 1$, we set $\psi_{\mathcal{T}_k}$ the vector of $\mathbb{R}^{\mathcal{T}_k}$ as

$$\psi_L^n = \psi(x_L, t^n), \quad \forall L \in \overline{\mathfrak{M}}_k \cup \overline{\mathfrak{M}^\star}_k,$$

We then take $u_{\mathcal{T}} = \psi_{\mathcal{T}_k}^n$ in the formulation (2.14). We sum on all $n\geq 1$ and rearrange the summation into three parts

$$\mathcal{W}_k + \mathcal{X}_k + \mathcal{Y}_k = 0,$$

where

$$\mathcal{W}_k = \sum_{n=1}^{N} \big[\!\big[p_{\mathcal{T}_k}^n - p_{\mathcal{T}_k}^{n-1}, \psi_{\mathcal{T}_k}^n \big]\!\big]_{\mathcal{T}_k},$$

$$\mathcal{X}_k = \frac{1}{2}\sum_{n=1}^{N} \delta t_k \sum_{\mathcal{D}_{\sigma,\sigma^\star}\in\mathfrak{S}_k} \beta(p_\sigma^n) F_{A,\sigma}(\beta(p_{\mathcal{T}_k}^n))(\psi_A^n - \psi_B^n) + \beta(p_{\sigma^\star}^n) F_{A^\star,\sigma^\star}(\beta(p_{\mathcal{T}_k}^n))(\psi_{A^\star}^n - \psi_{B^\star}^n),$$

$$\mathcal{Y}_k = \lambda \sum_{n=1}^{N} \delta t_k \big[\!\big[\mathcal{P}^{\mathcal{T}_k} \log\big(\beta(p_{\mathcal{T}_k}^n)\big), \psi_{\mathcal{T}_k}^n \big]\!\big]_{\mathcal{T}_k}.$$

First notice that $\psi_{\mathcal{T}_k}^N = 0$. Using a discrete integration by parts in time gives

$$\begin{aligned}\mathcal{W}_k &= -\big[\!\big[p_{\mathcal{T}_k}^0, \psi_{\mathcal{T}_k}^0 \big]\!\big]_{\mathcal{T}_k} - \sum_{n=1}^{N} \big[\!\big[p_{\mathcal{T}_k}^{n-1}, \psi_{\mathcal{T}_k}^n - \psi_{\mathcal{T}_k}^{n-1} \big]\!\big]_{\mathcal{T}_k} \\ &= -\int_\Omega p^0 \psi_{h_k,\delta t_k}(\cdot,0)\,\mathrm{d}x - \int_{Q_{t_f}} p_{h_k,\delta t_k}(\cdot,-\delta t_k)\left(\frac{\psi_{h_k,\delta t_k} - \psi_{h_k,\delta t_k}(\cdot,-\delta t_k)}{\delta t_k}\right)\mathrm{d}x\,\mathrm{d}t.\end{aligned}$$

Owing to the smoothness of the test function ψ, one has

$$\psi_{h_k,\delta t_k}(\cdot,0) \xrightarrow[k\to\infty]{} \psi(\cdot,0) \quad \text{and} \quad \left(\frac{\psi_{h_k,\delta t_k}-\psi_{h_k,\delta t_k}(\cdot,-\delta t_k)}{\delta t_k}\right) \xrightarrow[k\to\infty]{} \frac{\partial\psi}{\partial t},$$

uniformly on Ω and Q_{t_f} respectively. Since $p_{h_k,\delta t_k}$ converges strongly towards p in $L^1(Q_{t_f})$ we use the Fréchet-Kolmogorov compactness theorem to claim that $p_{h_k,\delta t_k}(\cdot,-\delta t_k)$ converges strongly towards p in $L^1(Q_{t_f})$. We then infer that

$$\mathcal{W}_k \xrightarrow[k\to\infty]{} -\int_\Omega p^0\psi(\cdot,0)\,\mathrm{d}x - \int_{Q_{t_f}} p\frac{\partial\psi}{\partial t}\,\mathrm{d}x\,\mathrm{d}t.$$

Let us move on to the convergence study of the diffusion term $\mathcal{X}_k$. We can not usually pass to the limit in terms like $\mathcal{X}_k$ directly. It is customary to introduce an additional diffusion term written in the integral form which converges to its continuous counterpart. Then, the latter must match the limit of $\mathcal{X}_k$. To this purpose, we first define $\beta_{\mathfrak{S}_k,\delta t_k}$ as a piecewise constant function on the diamond mesh and in time such that

$$\begin{aligned} &p^n_{\mathcal{D}}(x,t) = \beta^{-1}\Big(\frac{1}{2}\big(\beta(p^n_\sigma)+\beta(p^n_{\sigma^\star})\big)\Big), \quad \forall (x,t)\in\mathcal{D}\times(t^{n-1},t^n],\\ &\beta_{\mathfrak{S}_k,\delta t_k}(x,t) = \beta(p^n_{\mathcal{D}}(x,t)), \quad \forall (x,t)\in\mathcal{D}\times(t^{n-1},t^n]. \end{aligned}$$

Let us also consider

$$\widetilde{\mathcal{X}}_k = \frac{1}{2}\sum_{n=1}^N \delta t_k \sum_{\mathcal{D}_{\sigma,\sigma^\star}\in\mathfrak{S}_k} \beta(p^n_{\mathcal{D}})\Big(F_{A,\sigma}(\beta(p^n_{\mathcal{T}_k}))(\psi^n_A-\psi^n_B)+F_{A^\star,\sigma^\star}(\beta(p^n_{\mathcal{T}_k}))(\psi^n_{A^\star}-\psi^n_{B^\star})\Big).$$

Thanks to the discrete flux expression given in (2.9) and the discrete gradient mentioned in (2.4) we rewrite $\widetilde{\mathcal{X}}_k$ in the compact form

$$\widetilde{\mathcal{X}}_k = \int_{Q_{t_f}} \beta_{\mathfrak{S}_k,\delta t_k}\Lambda_{\mathfrak{S}_k}\nabla_{\mathfrak{S}_k,\delta t_k}\beta(p_{\mathcal{T}_k})\cdot\nabla_{\mathfrak{S}_k,\delta t_k}\psi_{\mathcal{T}_k}\,\mathrm{d}x\,\mathrm{d}t.$$

The sequence $\Lambda_{\mathfrak{S}_k}$ converges a.e. to Λ. From the regularity of ψ, the sequence $\nabla_{\mathfrak{S}_k,\delta t_k}\psi_{\mathcal{T}_k}$ converges uniformly towards $\nabla\psi$. In light of (4.4), the weak convergence of $\nabla_{\mathfrak{S}_k,\delta t_k}\beta(p_{\mathcal{T}_k})$ towards $\nabla\beta(p)$ holds true. To conclude that

$$\widetilde{\mathcal{X}}_k \xrightarrow[k\to\infty]{} \int_{Q_{t_f}} \beta(p)\Lambda\nabla\beta(p)\cdot\nabla\psi\,\mathrm{d}x\,\mathrm{d}t,$$

it is sufficient to show that

$$\beta_{\mathfrak{S}_k,\delta t_k} \xrightarrow[k\to\infty]{} \beta(p) \quad \text{strongly in } L^2(Q_{t_f}).$$

To this end, we develop the L^2 norm of $\beta_{\mathfrak{S}_k,\delta t_k}-\beta(p_{h_k,\delta t_k})$ on the both halves of each diamond cell and we employ Corollary 3.1 to deduce

$$\begin{aligned} 2\left\|\beta_{\mathfrak{S}_k,\delta t_k}-\beta(p_{h_k,\delta t_k})\right\|_{L^2(Q_{t_f})} &\le \left\|\widehat{\beta}_{\mathfrak{S}_k,\delta t_k}-\beta(p_{\mathfrak{M}_k,\delta t_k})\right\|_{L^2(Q_{t_f})} + \left\|\widehat{\beta}^\star_{\mathfrak{S}_k,\delta t_k}-\beta(p_{\overline{\mathfrak{M}^\star}_k,\delta t_k})\right\|_{L^2(Q_{t_f})}\\ &\le Ch_k \xrightarrow[k\to\infty]{} 0. \end{aligned}$$

Therefore $\beta_{\mathfrak{S}_k,\delta t_k}$ converges to $\beta(p)$ in the L^2 norm using (4.5). Let us next establish that $\mathcal{X}_k$ and $\widetilde{\mathcal{X}}_k$ are asymptotically identical. We compute

$$\begin{aligned} \left|\mathcal{X}_k-\widetilde{\mathcal{X}}_k\right| \le \frac{1}{2}\sum_{n=1}^N \delta t_k \sum_{\mathcal{D}_{\sigma,\sigma^\star}\in\mathfrak{S}_k} &\left|\Big(\beta(p^n_\sigma)-\beta(p^n_{\mathcal{D}})\Big)F_{A,\sigma}(\beta(p^n_{\mathcal{T}_k}))(\psi^n_A-\psi^n_B)\right|\\ &+\left|\Big(\beta(p^n_{\sigma^\star})-\beta(p^n_{\mathcal{D}})\Big)F_{A^\star,\sigma^\star}(\beta(p^n_{\mathcal{T}_k}))(\psi^n_{A^\star}-\psi^n_{B^\star})\right|. \end{aligned}$$

Reproducing similar calculations used already to estimate $\mathcal{Z}_2$ in (4.2) we get

$$\left|\mathcal{X}_k - \widetilde{\mathcal{X}}_k\right| \leq C \left\|\nabla\psi\right\|_{L^\infty(Q_{t_f})} \left\|\nabla_{\mathfrak{S}_k,\delta t_k}\beta(p_{\mathcal{T}_k})\right\|_{L^2(Q_{t_f})^2} \times \left(\left\|\widehat{\beta}_{\mathfrak{S}_k,\delta t_k} - \beta_{\mathfrak{S}_k,\delta t_k}\right\|_{L^2(Q_{t_f})} + \left\|\widehat{\beta}^{\star}_{\mathfrak{S}_k,\delta t_k} - \beta_{\mathfrak{S}_k,\delta t_k}\right\|_{L^2(Q_{t_f})}\right).$$

The energy estimate (3.2) conducts us to

$$\left|\mathcal{X}_k - \widetilde{\mathcal{X}}_k\right| \leq C \left(\left\|\widehat{\beta}_{\mathfrak{S}_k,\delta t_k} - \beta_{\mathfrak{S}_k,\delta t_k}\right\|_{L^2(Q_{t_f})} + \left\|\widehat{\beta}^{\star}_{\mathfrak{S}_k,\delta t_k} - \beta_{\mathfrak{S}_k,\delta t_k}\right\|_{L^2(Q_{t_f})}\right).$$

Note that $\widehat{\beta}_{\mathfrak{S}_k,\delta t_k}$ and $\widehat{\beta}^{\star}_{\mathfrak{S}_k,\delta t_k}$ converge strongly towards $\beta(p)$ in $L^2(Q_{t_f})$ according to Corollary 3.1. Consequently

$$\left|\mathcal{X}_k - \widetilde{\mathcal{X}}_k\right| \xrightarrow[k\to\infty]{} 0.$$

In order to finish up the proof of Theorem 4.1 it remains to prove that the limit of the penalty term equals 0. We combine the Cauchy-Schwarz inequality, the a priori estimate (3.2), the smoothness of ψ and the fact that $\eta \in (0,2)$ to obtain

$$\begin{aligned}|\mathcal{Y}_k| &\leq \lambda \left(\sum_{n=1}^{N} \delta t_k \left[\!\left[\mathcal{P}^{\mathcal{T}_k} \log\left(\beta(p^n_{\mathcal{T}_k})\right), \log(\beta(p^n_{\mathcal{T}_k}))\right]\!\right]_{\mathcal{T}_k}\right)^{\frac{1}{2}} \left(\sum_{n=1}^{N} \delta t_k \left[\!\left[\mathcal{P}^{\mathcal{T}_k}\psi^n_{\mathcal{T}_k}, \psi^n_{\mathcal{T}_k}\right]\!\right]_{\mathcal{T}_k}\right)^{\frac{1}{2}} \\ &\leq \frac{C}{h_k^{\eta/2}} \left\|\psi_{\mathfrak{M}_k,\delta t_k} - \psi_{\overline{\mathfrak{M}^\star}_k,\delta t_k}\right\|_{L^2(\Omega)} \leq C h_k^{1-(\eta/2)} \left\|\nabla\psi\right\|_{L^\infty(Q_{t_f})} \leq C h_k^{1-(\eta/2)} \xrightarrow[k\to\infty]{} 0.\end{aligned}$$

In conclusion, p is a weak solution to (1.1)-(1.3) in the sense of Definition 1.1. □

5 Computational results

In this section, we present and discuss various numerical examples for the resolution of the nonlinear diffusion problem (1.1). The objective is to enlighten the robustness and accuracy of the proposed scheme on possibly distorted and poor quality meshes. For all the tests, the Newton method is implemented to solve the nonlinear algebraic system. We consider the maximum of the smallest value of the initial guess as 10^{-16}. This allows to avoid the singularity of the involved log function. The exponent η is set to $\eta = 1$.

We fix the domain of computation to $\Omega = (0,1)^2$. It is discretized using a sequence of randomly perturbed and Kershaw meshes. The first element for each category is drawn on Figure 2. The time step is proportional to square of the mesh size so as to assess space accuracy of the method. To simplify the identification of analytical solutions, the matrix Λ is diagonal as follows

$$\Lambda = \begin{pmatrix} a_x & 0 \\ 0 & a_y \end{pmatrix}.$$

We will denote Er2p the errors between the exact and the numerical solutions in the sense of $L^\infty(0,t_f,L^2(\Omega))$-norm :

$$\text{Er2p} = \left\|p_a - p_{h,\delta t}\right\|_{L^\infty(0,t_f,L^2(\Omega))}.$$

The corresponding convergence rates will be designated by τ_p. Similarly, we consider the difference between the analytical and approximate gradient of the solutions denoted by Er2Gp using the norm of $L^2(Q_{t_f})^2$:

$$\text{Er2Gp} = \left\|\nabla p_a - \nabla_{\mathfrak{S},\delta t} p_{\mathcal{T}}\right\|_{L^2(Q_{t_f})^2}.$$

In this case, the order of convergence will be denoted by τ_{Gp}.

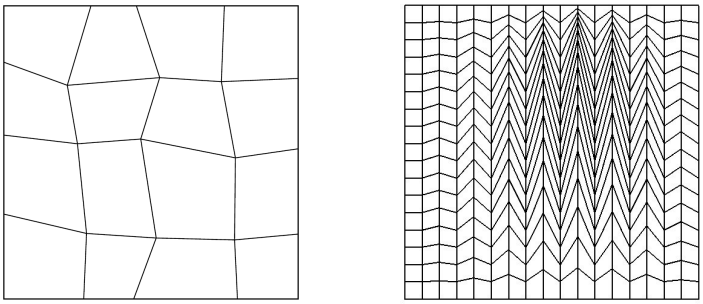

Figure 2: First deformed quadrilateral mesh on left and first Kershaw mesh on right.

5.1 Test case 1

This first representative experiment deals with the classical heat problem. After the nonlinear transformation (1.5), the heat equation can be written like

$$\frac{\partial p}{\partial t} - 2\,\mathrm{div}\,\sqrt{p}\Lambda\nabla\sqrt{p} = 0, \tag{5.1}$$

complemented with the zero-flux boundary condition. We define the one-dimensional analytical solution by

$$p_a(x,y,t) = \frac{1}{2}\Big(1+\cos(\pi x)\Big)e^{-\pi^2 a_x t}.$$

The initial condition matches this solution at $t = 0$. The simulation time is $t_f = 0.2$. The domain is anisotropic with $a_x = 1$ and $a_y = 1000$.

We first would like to stress that the additional penalty in the proposed scheme is useless numerically. In theory, it was introduced to reinforce the convergence of the primal and the dual solution reconstructions $p_{\mathfrak{M},\delta t}$ and $p_{\overline{\mathfrak{M}^\star},\delta t}$ towards the same limit. This fact holds from a numerical viewpoint. Let us then run the implemented scheme on the sequence of the randomly deformed meshes. We compute $||p_{\mathfrak{M},\delta t} - p_{\overline{\mathfrak{M}^\star},\delta t}||_{L^2(Q_{t_f})}$ for two values of λ. The results are written in Table 1. According to this table we observe a rate of order one between the approximation of the solution on the primal mesh and on the dual mesh independently of the coefficient λ. By virtue of this, the penalty parameter λ is fixed to 0 in the remaining part of this section.

		$\lambda = 0$		$\lambda = 1$	
$\#\mathcal{T}$	δt	$\|\|p_{\mathfrak{M},\delta t} - p_{\overline{\mathfrak{M}^\star},\delta t}\|\|_2$	rate	$\|\|p_{\mathfrak{M},\delta t} - p_{\overline{\mathfrak{M}^\star},\delta t}\|\|_2$	rate
57	0.12 E-01	0.505 E-01	-	0.506 E-01	-
177	0.30 E-02	0.190 E-01	1.454	0.191 E-01	1.454
609	0.84 E-03	0.931 E-02	1.117	0.931 E-02	1.118
2241	0.22 E-03	0.446 E-02	1.102	0.447 E-02	1.103
8577	0.37 E-04	0.217 E-02	0.809	0.218 E-02	0.810

Table 1: Evaluation of $||p_{\mathfrak{M},\delta t} - p_{\overline{\mathfrak{M}^\star},\delta t}||_{L^2(Q_{t_f})}$ with and without penalty.

Let us now return to evaluate the accuracy of our discretization for both the discrete solution and its discrete gradient. The results of their numerical convergence are shown on Tables 2-3 for the randomly distorted quadrilateral and Kershaw meshes respectively. From the tables, both approaches preserve the second-order accuracy for the solution. This optimal accuracy is not affected by the distortion of the mesh nor the anisotropy. The convergence order for the gradient is greater than 1.3 on the considered refined meshes. The last column of the same tables shows that the nonlinear scheme produces a positive solution, which confirms the point of Proposition 3.2. This is not the case of the standard linear DDFV schemes where overshoots and undershoots could occur, see the test case of Subsection 5.4.

$\#\mathcal{T}$	δt	Er2p	τ_p	Er2Gp	τ_{Gp}	p_{min}
57	0.12 E-01	0.154 E-01	-	0.374 E-01	-	0.51 E-01
177	0.30 E-02	0.392 E-02	2.039	0.107 E-01	1.860	0.14 E-01
609	0.84 E-03	0.104 E-02	2.066	0.389 E-02	1.583	0.12 E-08
2241	0.22 E-03	0.268 E-03	2.039	0.163 E-02	1.307	0.50 E-10
8577	0.37 E-04	0.605 E-04	1.677	0.382 E-03	1.635	0.83 E-13

Table 2: Test case 1 results using the sequence of randomly deformed meshes.

$\#\mathcal{T}$	δt	Er2p	τ_p	Er2Gp	τ_{Gp}	p_{min}
681	0.73 E-02	0.497 E-02	-	0.212 E-01	-	0.33 E-01
2517	0.18 E-02	0.127 E-02	1.965	0.588 E-02	1.850	0.21 E-07
5509	0.82 E-03	0.568 E-03	1.990	0.258 E-02	2.027	0.17 E-07
9657	0.46 E-03	0.320 E-03	1.996	0.159 E-02	1.307	0.97 E-09
14961	0.29 E-03	0.204 E-03	1.998	0.100 E-02	1.676	0.89 E-09

Table 3: Test case 1 results using the sequence of Kershaw meshes.

5.2 Test case 2

The following example addresses the numerical errors as well as a discrete maximum principle for the investigated finite volume scheme in the case of a nonlinear polynomial expression of $\mu(p)$. Then, the diffusion function is given by $\mu(p) = 3p^2$. Consequently, one has $\beta(p) = \sqrt{2}p^{3/2}$. We set the final time to $t_f = 0.1$. We take into account a slightly anisotropic diffusion with $a_x = 0.1$ and $a_y = 1$. We therefore consider the analytical solution

$$p_a(x, y, t) = 5t\big(1 + \cos(\pi x)\big), \tag{5.2}$$

subject to the initial boundary value problem (1.1)-(1.3) leading to a source term which is nonnegative. On the other hand, this solution maintains the zero-flux boundary constraint. The initial condition is in accordance with (5.2). As in the first test, the obtained results are reported in Tables 4-5.

Inspecting these tables, we note again a super-convergence on the solution and better convergence rates on the gradient. The implemented nonlinear scheme does not violate the discrete maximum principle. Thereby, the accuracy of our strategy is not severely sensible to polynomial nonlinearities, the anisotropy and the mesh quality.

$\#\mathcal{T}$	δt	Er2p	τ_p	Er2Gp	τ_{Gp}	p_{min}
57	0.12 E-01	0.360 E-02	-	0.489 E-01	-	0.10 E-12
177	0.30 E-02	0.855 E-03	2.140	0.125 E-01	2.028	0.30 E-14
609	0.84 E-03	0.372 E-03	1.297	0.400 E-02	1.778	0.41 E-15
2241	0.22 E-03	0.101 E-03	1.956	0.150 E-02	1.468	0.10 E-15
8577	0.37 E-04	0.177 E-04	1.962	0.356 E-03	1.626	0.10 E-15

Table 4: Test case 2 results using the sequence of randomly deformed meshes.

5.3 Test case 3

In this third example we increase the nonlinearities seriousness and look at their impact on the behavior of solutions to the studied finite volume scheme. To this purpose, we set

$$\mu(p) = \frac{4p\log(1 + p^2)}{1 + p^2},$$

$\#\mathcal{T}$	δt	Er2p	τ_p	Er2Gp	τ_{Gp}	p_{min}
681	0.73 E-02	0.330 E-03	-	0.254 E-01	-	0.81 E-13
2517	0.18 E-02	0.109 E-03	1.592	0.650 E-02	1.971	0.96 E-15
5509	0.82 E-03	0.508 E-04	1.893	0.289 E-02	1.993	0.11 E-15
9657	0.46 E-03	0.290 E-04	1.952	0.163 E-02	1.997	0.10 E-15
14961	0.29 E-03	0.188 E-04	1.928	0.104 E-02	1.992	0.10 E-15

Table 5: Test case 2 results using the sequence of Kershaw meshes.

yielding $\beta(p) = \log(1 + p^2)$. We consider the anisotropy $a_x = 0.1$ and $b_x = 10$. We moreover manufacture the exact solution to be

$$p_a(x, y, t) = 90tx^2(1 - x)^2.$$

It also respects the zero-flux boundary condition. The initial solution is taken as $p^0 = p_a(\cdot, \cdot, 0)$. Its substitution in the problem (1.1)-(1.3) leads to a nonnegative source contribution. The numerical results of the proposed nonlinear algorithm are given in Tables 6-7.

It is observed that the designed nonlinear scheme produces an approximate solution that converges to the continuous one with a rate of second order. Notice that the minimum of the computed solution is also positive. Concerning the errors of the gradients, convergence rates are much improved on the Kershaw meshes than the randomly deformed ones. Here again, this example illustrates that our methodology is capable to handle severe nonlinearities even on distorted meshes.

$\#\mathcal{T}$	δt	Er2p	τ_p	Er2Gp	τ_{Gp}	p_{min}
57	0.12 E-01	0.338 E-02	-	0.735 E-01	-	0.46 E-08
177	0.30 E-02	0.856 E-03	2.047	0.193 E-01	1.988	0.11 E-12
609	0.84 E-03	0.318 E-03	1.544	0.669 E-02	1.656	0.11 E-15
2241	0.22 E-03	0.106 E-03	1.639	0.283 E-02	1.288	0.10 E-15
8577	0.37 E-04	0.183 E-04	1.989	0.702 E-03	1.575	0.10 E-15

Table 6: Test case 3 results using the sequence of randomly deformed meshes.

$\#\mathcal{T}$	δt	Er2p	τ_p	Er2Gp	τ_{Gp}	p_{min}
681	0.73 E-02	0.198 E-03	-	0.294 E-01	-	0.93 E-12
2517	0.18 E-02	0.625 E-04	1.664	0.750 E-02	1.972	0.13 E-15
5509	0.82 E-03	0.288 E-04	1.909	0.334 E-02	1.994	0.10 E-15
9657	0.46 E-03	0.163 E-04	1.967	0.188 E-02	1.998	0.10 E-15
14961	0.29 E-03	0.106 E-04	1.942	0.121 E-02	1.992	0.10 E-15

Table 7: Test case 3 results using the sequence of Kershaw meshes.

5.4 Test case 4

In this last experiment, we compare the behavior of the approximate solution computed by the proposed nonlinear scheme to the one provided by the classical linear DDFV discretization in the case of the heat equation with a low regular initialization function. The initial condition is then taken to be

$$p^0 = \begin{cases} 1 & \text{on} \quad \Omega_0 = [0.3, 0.7] \times [0.3, 0.7] \\ 0 & \text{on} \quad \Omega \setminus \Omega_0 \end{cases}.$$

In such a situation we do not have access to the exact solution. It is however expected to be nonnegative. The domain Ω is covered by the cells of the third randomly deformed mesh. We consider the problem

with the anisotropy $a_x = 1$ and $a_y = 0.1$. The final time is chosen as $t_f = 0.02$. We fix the time step to $\delta t = 0.001$.

We perform two tests with this identical set up. In the first run, we determine the numerical solution to the classical linear DDFV scheme, for the heat problem, by solving the linear system

$$\frac{|A|}{\delta t}(p_A^n - p_A^{n-1}) - \sum_{\mathcal{D}_{\sigma,\sigma^\star} \in \mathcal{D}_A} |\sigma| \, \Lambda \nabla_{\mathcal{D}} p_{\mathcal{T}}^n \cdot \mathbf{n}_{\sigma,A} = 0, \quad \forall A \in \mathfrak{M}, \tag{5.3}$$

$$\frac{|A^\star|}{\delta t}(p_{A^\star}^n - p_{A^\star}^{n-1}) - \sum_{\mathcal{D}_{\sigma,\sigma^\star} \in \mathcal{D}_{A^\star}} |\sigma^\star| \, \Lambda \nabla_{\mathcal{D}} p_{\mathcal{T}}^n \cdot \mathbf{n}_{\sigma^\star,A^\star} = 0, \quad \forall A^\star \in \overline{\mathfrak{M}^\star}, \tag{5.4}$$

$$|\sigma| \, \Lambda \nabla_{\mathcal{D}} p_{\mathcal{T}}^n \cdot \mathbf{n}_{\sigma,A} = 0, \quad \forall A \in \partial\mathfrak{M}. \tag{5.5}$$

Recall that the linear DDFV method is also accurate of second order [39]. In the second run, the numerical solution is obtained by executing the alternative nonlinear algorithm (2.10)-(2.13). The results of the simulation are given on Figure 3. The latter shows the cross section of the calculated solution at the point $(0, 0.2)$ for the instants $t \in \{3.10^{-3}, 6.10^{-3}, 8.10^{-3}, 1.10^{-2}\}$. The left sub-figure exhibits the result of the linear scheme (5.3)-(5.5). It is clearly seen that the linear discretization forms severe peaks that go under 0. This defect can not be evaded or disregarded since it engenders critical deviation on the diffusion process. This kind of oscillation is a standard fact in the literature of the DDFV approach. To overcome this problem, we use the nonlinear version of the scheme (2.10)-(2.13). The results are presented on the right sub-figure. This strategy produces no oscillation and the solution honors its lower bound which is 0. Therefore, the proposed nonlinear scheme is more robust and stable than the well-known linear DDFV approximation.

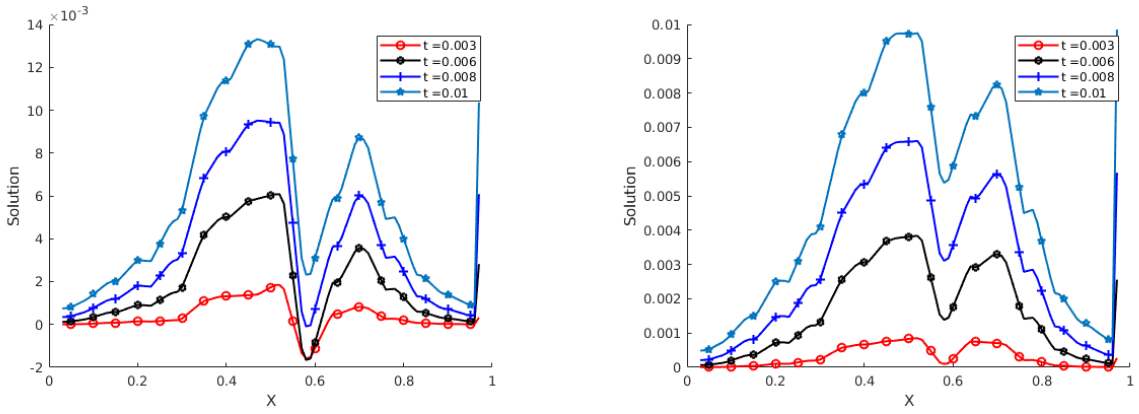

Figure 3: Results for the linear DDFV scheme (5.3)-(5.5) (left) and nonlinear formulation (2.10)-(2.13) (right).

6 Conclusion

In this work we proposed and studied a new nonlinear discrete duality finite volume method for the discretization of parabolic equations. The objective is obtain a stable, convergent and accurate strategy which works also on general data and meshes defined by the physics of the problem. In addition to accuracy quests, a huge focus has been paid on assembling key properties referred to as coercivity and positivity. To achieve this we have suggested a chief idea for the approximation of the fluxes. It resides in the centered fractional scheme for the diffusion function. By taking an appropriate nonlinear discrete test function we control some energy estimates. The latter have particularly ensured the existence of positive approximate solutions. Thanks to a compactness criterion, the convergence of the numerical scheme has been established. Numerical simulation has been performed and exhibited good results. The accuracy is of second order on severe nonlinearities and the solution is still positive even on distorted meshes. This confirms the efficiency and the robustness of the proposed methodology.

Acknowledgments: The author would like to thank Boris Andreianov for the reading and for his pertinent comments that improved the quality of the paper. This contribution was supported by the National Research Agency of France (CHARMS ANR project, ANR-16-CE06-0009).

The author would also like to acknowledge the Reviewers for their valuable comments.

References

[1] I. Aavatsmark, T. Barkve, Ø. Bøe, and T. Mannseth. Discretization on non-orthogonal, quadrilateral grids for inhomogeneous, anisotropic media. *Journal of Computational Physics*, 127(1):2–14, 1996.

[2] M. Afif and B. Amaziane. Convergence of finite volume schemes for a degenerate convection–diffusion equation arising in flow in porous media. *Computer Methods in Applied Mechanics and Engineering*, 191(46):5265–5286, 2002.

[3] H. W. Alt and S. Luckhaus. Quasilinear elliptic-parabolic differential equations. *Mathematische Zeitschrift*, 183(3):311–341, 1983.

[4] G. Amiez and P.-A. Gremaud. On a numerical approach to Stefan-like problems. *Numerische Mathematik*, 59(1):71–89, 1991.

[5] B. Andreianov, M. Bendahmane, and K. H. Karlsen. Discrete duality finite volume schemes for doubly nonlinear degenerate hyperbolic-parabolic equations. *Journal of Hyperbolic Differential Equations*, 7(01):1–67, 2010.

[6] B. Andreianov, M. Bendahmane, and M. Saad. Finite volume methods for degenerate chemotaxis model. *Journal of Computational and Applied Mathematics*, 235(14):4015–4031, 2011.

[7] B. Andreianov, F. Boyer, and F. Hubert. Discrete duality finite volume schemes for Leray-Lions-type elliptic problems on general 2D meshes. *Numerical Methods for Partial Differential Equations*, 23(1):145–195, 2007.

[8] B. Andreianov, C. Cancès, and A. Moussa. A nonlinear time compactness result and applications to discretization of degenerate parabolic–elliptic PDEs. *Journal of Functional Analysis*, 273(12):3633–3670, 2017.

[9] T. Arbogast and M. F. Wheeler. A nonlinear mixed finite element method for a degenerate parabolic equation arising in flow in porous media. *SIAM Journal on Numerical Analysis*, 33(4):1669–1687, 1996.

[10] M. Bendahmane, Z. Khalil, and M. Saad. Convergence of a finite volume scheme for gas–water flow in a multi-dimensional porous medium. *Mathematical Models and Methods in Applied Sciences*, 24(01):145–185, 2014.

[11] M. Bessemoulin-Chatard. A finite volume scheme for convection–diffusion equations with nonlinear diffusion derived from the Scharfetter–Gummel scheme. *Numerische Mathematik*, 121(4):637–670, 2012.

[12] M. Bessemoulin-Chatard, C. Chainais-Hillairet, and F. Filbet. On discrete functional inequalities for some finite volume schemes. *IMA Journal of Numerical Analysis*, 35(3):1125–1149, 2015.

[13] V. I. Bogachev. *Measure theory*, volume 1. Springer Science & Business Media, 2007.

[14] F. Boyer and F. Hubert. Finite volume method for 2D linear and nonlinear elliptic problems with discontinuities. *SIAM Journal on Numerical Analysis*, 46(6):3032–3070, 2008.

[15] K. Brenner and R. Masson. Convergence of a vertex centred discretization of two-phase Darcy flows on general meshes. *International Journal on Finite Volumes*, 10:1–37, 2013.

[16] K. Brenner, R. Masson, and E. H. Quenjel. Vertex Approximate Gradient Discretization preserving positivity for two-phase Darcy flows in heterogeneous porous media. *Journal of Computational Physics*, 409:109357, 2020.

[17] F. Brezzi, K. Lipnikov, and M. Shashkov. Convergence of the mimetic finite difference method for diffusion problems on polyhedral meshes. *SIAM Journal on Numerical Analysis*, 43(5):1872–1896, 2005.

[18] C. Cancès, C. Chainais-Hillairet, and S. Krell. Numerical analysis of a nonlinear free-energy diminishing Discrete Duality Finite Volume scheme for convection diffusion equations. *Computational Methods in Applied Mathematics*, 18(3):407–432, 2018.

[19] C. Cancès and C. Guichard. Convergence of a nonlinear entropy diminishing control volume finite element scheme for solving anisotropic degenerate parabolic equations. *Mathematics of Computation*, 85(298):549–580, 2016.

[20] C. Cancès and C. Guichard. Numerical analysis of a robust free energy diminishing finite volume scheme for parabolic equations with gradient structure. *Foundations of Computational Mathematics*, 17(6):1525–1584, 2017.

[21] C. Chainais-Hillairet and J. Droniou. Finite-volume schemes for noncoercive elliptic problems with Neumann boundary conditions. *IMA Journal of Numerical analysis*, 31(1):61–85, 2011.

[22] C. Chainais-Hillairet, S. Krell, and A. Mouton. Convergence analysis of a DDFV scheme for a system describing miscible fluid flows in porous media. *Numerical Methods for Partial Differential Equations*, 31(3):723–760, 2015.

[23] G. Chavent and J. Jaffré. *Mathematical models and finite elements for reservoir simulation: single phase, multiphase and multicomponent flows through porous media*, volume 17. North-Holland, Amsterdam, Stud. Math. Appl. edition, 1986.

[24] Y. Coudière and F. Hubert. A 3D discrete duality finite volume method for nonlinear elliptic equations. *SIAM Journal on Scientific Computing*, 33(4):1739–1764, 2011.

[25] Y. Coudière and G. Manzini. The discrete duality finite volume method for convection-diffusion problems. *SIAM Journal on Numerical Analysis*, 47(6):4163–4192, 2010.

[26] K. Domelevo and P. Omnes. A finite volume method for the Laplace equation on almost arbitrary two-dimensional grids. *ESAIM: Mathematical Modelling and Numerical Analysis*, 39(6):1203–1249, 2005.

[27] J. Droniou. Finite volume schemes for diffusion equations: introduction to and review of modern methods. *Mathematical Models and Methods in Applied Sciences*, 24(08):1575–1619, 2014.

[28] J. Droniou and R. Eymard. A mixed finite volume scheme for anisotropic diffusion problems on any grid. *Numerische Mathematik*, 105(1):35–71, 2006.

[29] J. Droniou, R. Eymard, T. Gallouët, C. Guichard, and R. Herbin. *The gradient discretisation method*, volume 82. Springer, 2018.

[30] C. Ebmeyer. Error estimates for a class of degenerate parabolic equations. *SIAM Journal on Numerical Analysis*, 35(3):1095–1112, 1998.

[31] R. Eymard, T. Gallouët, and R. Herbin. Finite volume methods. In *Handbook of Numerical Analysis*, volume 7, pages 713–1018. Elsevier, 2000.

[32] R. Eymard, T. Gallouët, and R. Herbin. Discretization of heterogeneous and anisotropic diffusion problems on general nonconforming meshes SUSHI: a scheme using stabilization and hybrid interfaces. *IMA Journal of Numerical Analysis*, 30(4):1009–1043, 2010.

[33] R. Eymard, T. Gallouët, D. Hilhorst, and Y. N. Slimane. Finite volumes and nonlinear diffusion equations. *ESAIM: Mathematical Modelling and Numerical Analysis*, 32(6):747–761, 1998.

[34] R. Eymard, C. Guichard, R. Herbin, and R. Masson. Vertex-centred discretization of multiphase compositional Darcy flows on general meshes. *Computational Geosciences*, 16(4):987–1005, 2012.

[35] R. Eymard, D. Hilhorst, and M. Vohralík. A combined finite volume–nonconforming/mixed-hybrid finite element scheme for degenerate parabolic problems. *Numerische Mathematik*, 105(1):73–131, 2006.

[36] M. Ghilani, E. H. Quenjel, and M. Saad. Positive control volume finite element scheme for a degenerate compressible two-phase flow in anisotropic porous media. *Computational Geosciences*, 23(1):55–79, 2019.

[37] M. Ghilani, E. H. Quenjel, and M. Saad. Positivity-preserving finite volume scheme for compressible two-phase flows in anisotropic porous media: The densities are depending on the physical pressures. *Journal of Computational Physics*, 407:109233, 2020.

[38] M. E. Gurtin and R. C. MacCamy. On the diffusion of biological populations. *Mathematical Biosciences*, 33(1-2):35–49, 1977.

[39] R. Herbin and F. Hubert. Benchmark on discretization schemes for anisotropic diffusion problems on general grids. In R. Eymard and J.-M. Herard, editors, *Finite Volumes for Complex Applications V*, pages 659–692. Wiley, 2008.

[40] F. Hermeline. A finite volume method for the approximation of diffusion operators on distorted meshes. *Journal of Computational Physics*, 160(2):481–499, 2000.

[41] D. Horstmann. From 1970 until present: the Keller–Segel model in chemotaxis and its consequences. *I. Jahresberichte DMV*, 105(3):103–165, 2003.

[42] M. Kaviany. *Principles of heat transfer in porous media*. Springer Science & Business Media, 2012.

[43] S. Krell. Stabilized DDFV schemes for Stokes problem with variable viscosity on general 2D meshes. *Numerical Methods for Partial Differential Equations*, 27(6):1666–1706, 2011.

[44] E. H. Quenjel. Analysis of accurate and stable finite volume scheme for anisotropic diffusion equations with drift. *Preprint*, 2019.

[45] E. H. Quenjel. Enhanced positive vertex-centered finite volume scheme for anisotropic convection-diffusion equations. *ESAIM: Mathematical Modelling and Numerical Analysis*, 54(2):591–618, 2020.

[46] E. H. Quenjel, M. Saad, M. Ghilani, and M. Bessemoulin-Chatard. Convergence of a positive nonlinear DDFV scheme for degenerate parabolic equations. *Calcolo*, 57(19), 2020.

[47] C. Verti. Numerical aspects of parabolic free boundary and hysteresis problems. In *Phase transitions and hysteresis*, pages 213–284. Springer-Verlag, 1994.